Dalton Transactions

ROYAL SOCIETY OF CHEMISTRY

PAPER

View Article Online
View Journal | View Issue

Cite this: *Dalton Trans.*, 2020, **49**, 11978

INSIGHTS into the structures adopted by titanocalix[6 and 8]arenes and their use in the ring opening polymerization of cyclic esters†

Orlando Santoro,[a] Mark R. J. Elsegood, *[b] Elizabeth V. Bedwell,[b] Jake A. Pryce[b] and Carl Redshaw *[a]

Interaction of p-*tert*-butylcalix[6]areneH$_6$, L^{1}H$_6$, with [TiCl$_4$] afforded the complex [Ti$_2$Cl$_3$(MeCN)$_2$(OH$_2$)(L^{1}H)][Ti$_2$Cl$_3$(MeCN)$_3$(L^{1}H)]·4.5MeCN (**1**·4.5MeCN), in which two pseudo-octahedral titanium centres are bound to one calix[6]arene. A similar reaction but employing THF resulted in the THF ring-opened product [Ti$_4$Cl$_2$(μ_3-O)$_2$(NCMe)$_2$(L)$_2$(O(CH$_2$)$_4$Cl)$_2$]·4MeCN (**2**·4MeCN), where LH$_4$ = p-*tert*-butylcalix[4]areneH$_4$. Interaction of L^{1}H$_6$ with [TiF$_4$] (3 equiv.) led, after work-up, to the complex [(TiF)$_2$(μ-F)L^{1}H]$_2$·6.5MeCN (**3**·6.5MeCN). Treatment of p-*tert*-butylcalix[8]areneH$_8$, L^{2}H$_8$, with [TiCl$_4$] led to the isolation of the complex [(TiCl)$_2$(TiClNCMe)$_2$(μ_3-O)$_2$(L^2)]·1.5MeCN (**4**·1.5MeCN). From a similar reaction, a co-crystallized complex [Ti$_4$O$_2$Cl$_4$(MeCN)$_2$(L^2)][Ti$_3$Cl$_6$(MeCN)$_5$(OH$_2$)(L^{2}H$_2$)]·H$_2$O·11MeCN (**5**·H$_2$O 11MeCN) was isolated. Extension of the L^{2}H$_8$ chemistry to [TiBr$_4$] afforded, depending on the stoichiometry, the complexes [(TiBr)$_2$(TiBrNCMe)$_2$(μ_3-O)$_2$(L^2)]·6MeCN (**6**·6MeCN) or [[Ti(NCMe)$_2$Br]$_2$[Ti(O)Br$_2$(NCMe)](L^2)]·7.5MeCN (**7**·7.5MeCN), whilst use of [TiF$_4$] afforded complexes containing Ca^{2+} and Na$^+$, thought to originate from drying agents, namely [Ti$_8$CaF$_{20}$(OH$_2$)Na$_2$(MeCN)$_4$(L^2)$_2$]·14MeCN (**8**·14MeCN), [Na(MeCN)$_2$][Ti$_8$CaF$_{20}$NaO$_{16}$(L^2)$_2$]·7MeCN (**9**·7MeCN) or [Na]$_6$[Ti$_8$F$_{20}$Na(MeCN)$_2$(L^2)][Ti$_8$F$_{20}$Na(MeCN)$_{0.5}$(L^2)]·15.5(C$_2$H$_3$N) (**10**·15.5MeCN). In the case of [TiI$_4$], the ladder [(TiI)$_2$(TiINCMe)$_2$(μ_3-O)$_2$(L^2)]·7.25CH$_2$Cl$_2$ (**11**·7.25CH$_2$Cl$_2$) was isolated. These complexes have been screened for their potential to act as catalysts in the ring opening polymerization (ROP) of ε-caprolactone (ε-CL), δ-valerolactone (δ-VL) and *rac*-lactide (*r*-LA), both in air and N$_2$. For ε-CL and δ-VL, moderate activity at 130 °C over 24 h was observed for **1**, **9** and **11**; for *r*-LA, only **1** exhibited reasonable activity. In the case of the co-polymerization of ε-CL with δ-VL, the complexes **1** and **11** afforded reasonable conversions and low molecular weight polymers, whilst **4**, **6**, and **9** were less effective. None of the complexes proved to be active in the co-polymerization of ε-CL and *r*-LA under the conditions employed herein.

Received 15th June 2020,
Accepted 7th August 2020

DOI: 10.1039/d0dt02130j

rsc.li/dalton

Introduction

Frameworks capable of binding multiple metal centres are of interest in catalysis given the potential for beneficial cooperative effects.[1] Our interest in this area has been, and remains, focused mostly around the use of the family of polyphenolic macrocycles called calix[*n*]arenes.[2] For the *n* = 4 system, namely *p-tert*-butylcalix[4]areneH$_4$ (LH$_4$), the tendency is to coordinate to only one metal centre *via* the four phenolic oxygens (the lower rim) and usually the macrocycle retains the cone conformation.[3] Of the larger calix[*n*]arenes, the *n* = 6 (L^{1}H$_6$) and 8 (L^{2}H$_8$) systems are attractive scaffolds given their availability; odd numbered calix[*n*]arenes are isolated in far lower yields.[4] However, the coordination chemistry of the larger calix[*n*]arenes remains relatively unexplored.[2,5] In the case of titanium, reports date back to the 1980s.[6] In our coordination studies employing different metals (*i.e.* tungsten and vanadium), we have had limited success for *n* = 6,[7] whilst previous work for *n* = 8 has shown that it is possible, *via* controlling the reaction stoichiometry, to incorporate selectively two, three, or four metal centres (W) at the lower rim.[8] Furthermore, the systems incorporating vanadium have exhibited high catalytic activities in the area of α-olefin polymerization.[9] In the area of ring opening polymerization (ROP) of cyclic esters, reports using metallocalix[*n*]arenes are scant. In

[a]*Plastics Collaboratory, Department of Chemistry and Biochemistry, The University of Hull, Cottingham Road, Hull, HU6 7RX, UK. E-mail: C.Redshaw@hull.ac.uk*
[b]*Chemistry Department, Loughborough University, Loughborough, Leicestershire, LE11 3TU, UK*

†Electronic supplementary information (ESI) available. CCDC 1973130–1973136, 1973364–1973366, 2009076, and 2009077. For ESI and crystallographic data in CIF or other electronic format see DOI: 10.1039/d0dt02130j

the case of tungstocalix[6 and 8]arenes, we observed how different sized calixarene rings and their associated conformations can drastically affect the catalytic activity for the ROP of ε-caprolactone (ε-CL).[10] More recently, McIntosh *et al.* reported preliminary studies on the use of the complex $[Ti_4(L^2)(On\text{-}Pr)_8(THF)_2]$ as a catalyst for the ROP of *rac*-lactide (*r*-LA) at 130 °C.[11] Other titanocalix[*n*]arene work in this area employs the de-*tert*-butylated $n = 4$ system (1,3-di-*n*-propylcalix[4]arene), with well-behaved ROP of *rac*-lactide observed when employing either microwave radiation or heat; the former method was beneficial to the rate of polymerization at the expense of control.[12] A related system, possessing *para*-NO_2 and *tert*-butyl groups at the upper-rim of the calix[4]arene was capable of the well-controlled ROP of L- and *r*-LA under solvent-free conditions.[13] Recently, we have tested the efficiency of known complexes of the type $[TiCl_2L(O)_2(OR)_2]$ (R = Me, *n*-Pr and *n*-pentyl), the Cl-bridged compound $\{[TiL(O)_3(OR)]_2(\mu\text{-}Cl)_2\}$ (R = *n*-decyl) and the monochloride complex [Ti(NCMe)ClL$(O)_3$(OMe)] in the ROP of several cyclic esters.[14] Although all complexes were found to be efficient for ROP, the monochloride species proved to be the best performing of the series. It is noteworthy that all catalysts were shown to be active even under aerobic conditions, without any significant activity loss. Moreover, titanocalix[4]arene species were shown to be better performing than other Ti-based benchmark catalysts (including a Ti-diphenolate compound), suggesting a positive effect of the calix[4]arene ligand on the catalyst efficiency. These limited studies suggest there is the potential for accessing both controllable and highly active ROP catalysts based on titanocalix[*n*]arenes with $n \geq 6$. Herein, we focus on titanocalix[6 and 8]arenes derived from interaction of the parent *p-tert*-butylcalix[6 and 8]arenes, namely $n = 6$ (L^1H_6) and $n = 8$ (L^2H_8)

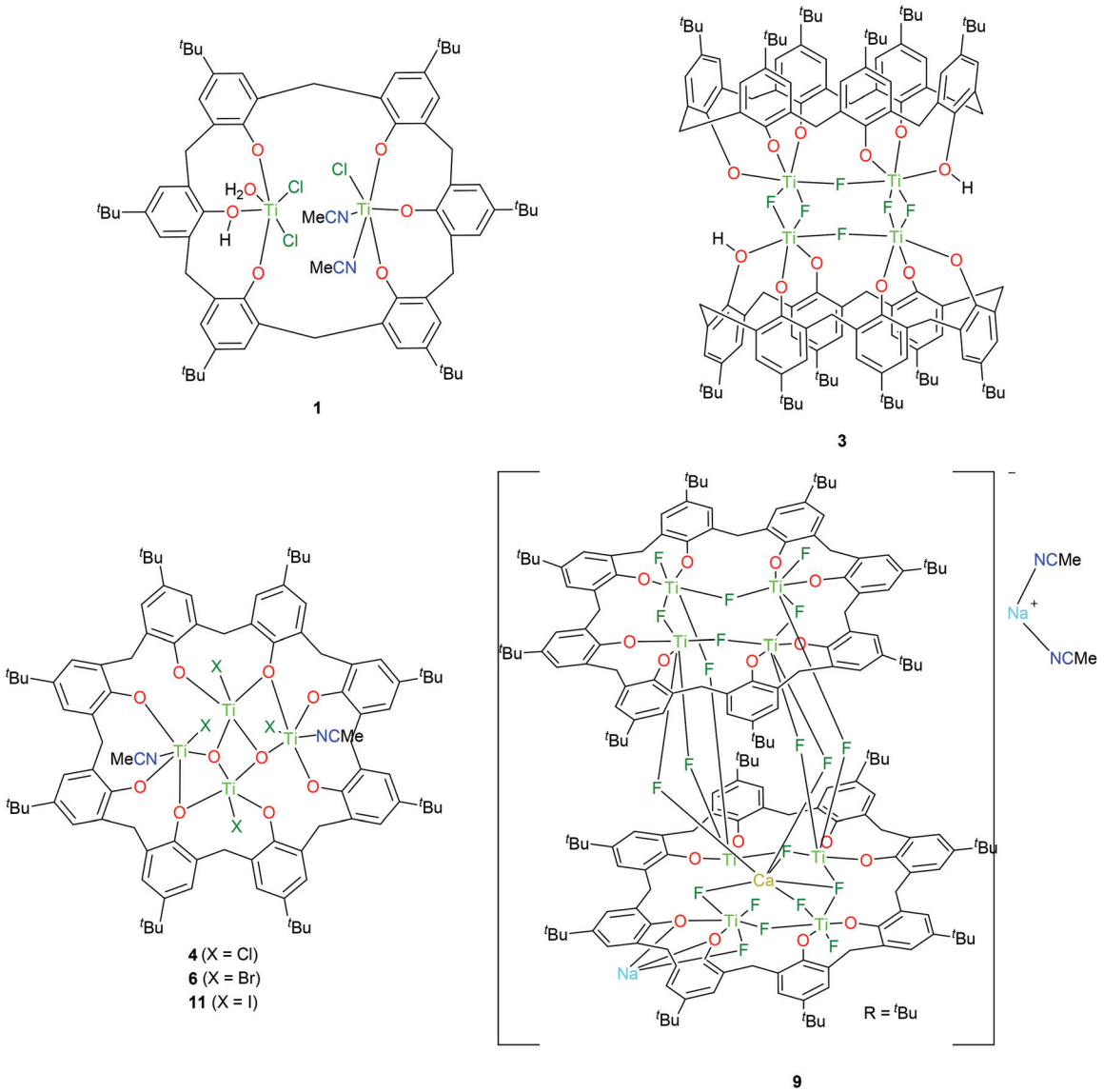

Chart 1 Titanocalix[6 and 8]arene complexes **1**, **3**, **4**, **6**, **9** and **11** prepared herein and tested as catalysts for the ROP of cyclic esters. (Complexes **2**, **5**, **7**, and **8** were not tested).

with the tetrahalides [TiX_4] (X = Cl, Br, F, I). A number of intriguing molecular structures (see Chart 1 and Fig. S1 and 2, ESI†) have been identified, and the complexes (not **2**, **5**, **7**, and **8**) have been screened for their ability to act as catalysts in the ROP of ε-CL, δ-valerolactone (δ-VL), and *r*-LA as well as for the copolymerization of ε-CL with δ-VL, and ε-CL with *r*-LA. We have recently reviewed the use of titanium diphenolates and titanocalix[4]arenes for both α-olefin polymerization and the ROP of cyclic esters.[15]

Results and discussion

Use of *p-tert*-butylcalix[6]areneH_6 L^1H_6

In the case of L^1H_6, where L^1 = *p-tert*-butylcalix[6]arene, interaction with two equivalents of [$TiCl_4$] afforded, after work-up (MeCN), the complex [$Ti_2Cl_3(MeCN)_2(OH_2)(L^1H)$] [$Ti_2Cl_3(MeCN)_3(L^1H)$]·4.5 MeCN (**1**·4.5 MeCN) as orange crystals on slow cooling to ambient temperature. In the IR spectrum, ν(CN) for both coordinated and free acetonitrile (2319/2308 and 2289 cm^{-1}, respectively) are observed. The molecular structure (CCDC 1973136†) of **1** is shown in Fig. 1, with selected bond lengths and angles given in the caption. The asymmetric unit contains two similar but unique molecules. In each case, the two pseudo-octahedral Ti(IV) ions are bound to an L^1H ligand *via* three phenolate oxygens to each titanium ion; the co-ordinated chlorides, acetonitrile molecules and water molecule are *facial*. In each molecule; the phenolic hydrogens on O(2) and O(2A) are retained, whilst Ti(1) is bonded to two Cl^- ions and one water molecule, Ti(1A) is bonded to two Cl^- ions and one MeCN molecule, and this is the chemical difference between the two unique metal complexes; Ti(2) and Ti(2A) are both bonded to one Cl^- ion and two MeCN molecules. There are hydrogen bonds between O(2)–H(2)···O(6A) and O(2A)–H(2A)···O(6). The retention of a phenolic hydrogen on L^1, allows for hydrogen bonding with an oxygen on the other molecule in the asymmetric unit, or the next pair along the chain. These pairs of molecules form infinite, H-bonded, zig-zag chains, in the *b*-direction (see Fig. S3, ESI†). The coordination of the metal to the calix[6]arene and the conformation adopted by the macrocycle are reminiscent of that observed for the group V complexes {[$M(NCMe)Cl_2]_2L^1$} (M = Nb, Ta).[16] When THF was employed as solvent, the orange/red complex [$Ti_4Cl_2(\mu_3\text{-}O)_2(NCMe)_2(L)_2(O(CH_2)_4Cl)_2]$·4MeCN (**2**·4MeCN) was isolated in low yield. Its molecular structure (CCDC 1973134†) is shown in Fig. S4 of the ESI.† The molecule lies on a centre of symmetry, and was refined as a 2-component twin (components 0.5431 : 0.4569(10)); component 2 rotated by 8.1802° around [−0.01 0.98 0.18] (reciprocal) or [0.20 0.92 0.33] (direct). The core of the complex can be described as two, singly vertex–vacant cubes, connected by a face, in which the Ti octahedra share edges. Both Ti(2) and Ti(2A) possess $O(CH_2)_4Cl$ groups. The main core of **2** was found to be similar to that of [$Ti(NCMe)(\mu_3\text{-}O)L(O)_4TiCl(O(CH_2)_4Cl)]_2$–2[$TiCl(NCMe)(L(O)_3(On\text{-}Pr))$]·11MeCN, a compound we have recently reported.[14] The formation of **2** is thought to involve the ring opening of the THF, which has been reported in the literature for a number of systems, particularly in the presence of Lewis acids and more recently in the reaction between boryl triflates and aryloxides.[17] The presence of a calix[4]arene rather than a calix[6]arene is thought to be due to the presence of a small amount of the n = 4 macrocycle in the batch of the precursor used. In the case of [TiF_4] (3 equiv.), reaction with L^1H_6 afforded, following extraction into MeCN, the orange/red complex [$(TiF)_2(\mu\text{-}F)L^1H]_2$·6.5MeCN (**3**·6.5MeCN). The molecular structure (CCDC 2009076†) is shown in Fig. 2, with selected bond lengths and angles given in the caption. The molecule lies on a centre of symmetry and so half is unique. Two distorted octahedral titanium centres are bound to each of the two L^1H macrocycles, the latter being linked by

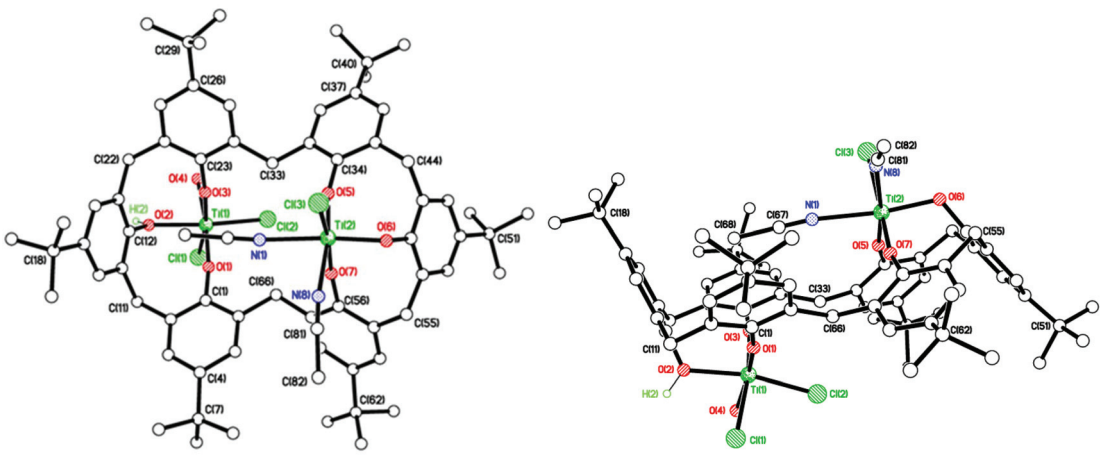

Fig. 1 Two views of the molecular structure of [$Ti_2Cl_3(MeCN)_2(OH_2)(L^1H)$][$Ti_2Cl_3(MeCN)_3(L^1H)$]·4.5 MeCN (**1**·4.5 MeCN). Solvent of crystallisation, minor components of disordered atoms, and most H atoms omitted for clarity. Selected bond lengths (Å) and angles (°): Ti(1)–O(1) 1.775(5), Ti(1)–O(2) 2.077(5), Ti(1)–O(3) 1.797(5), Ti(1)–O(4) 2.173(6), Ti(1)–Cl(1) 2.320(3), Ti(1)–Cl(2) 2.325(3), Ti(2)–O(5) 1.783(5), Ti(2)–O(6) 1.917(5), Ti(2)–O(7) 1.815(5), Ti(2)–N(1) 2.244(6), Ti(2)–N(8) 2.300(7), Ti(2)–Cl(3) 2.358(2); Ti(1)–O(1)–C(1) 172.4(5), Ti(1)–O(2)–C(12) 118.4(4), Ti(1)–O(3)–C(23) 159.9(4), Ti(2)–O(5)–C(34) 165.5(5), Ti(2)–O(6)–C(45) 117.5(4), Ti(2)–O(7)–C(56) 161.3(5).

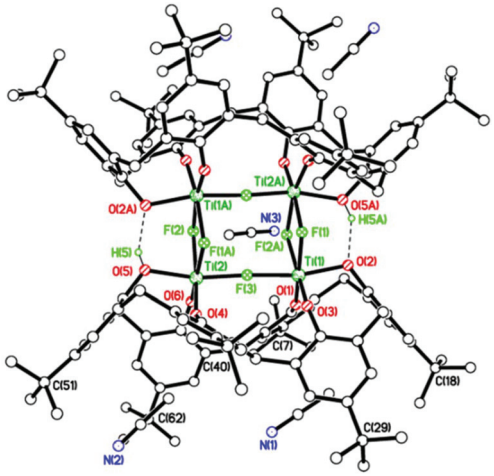

Fig. 2 Molecular structure of $[(TiF)_2(\mu\text{-}F)L^1H]_2\cdot 6.5MeCN$ (**3**·6.5MeCN). Most H atoms, minor components of disordered atoms, and most solvent molecules of crystallisation omitted for clarity. Selected bond lengths (Å) and angles (°): Ti(1)–O(1) 1.788(3), Ti(1)–O(2) 1.968(3), Ti(1)–O(3) 1.783(3), Ti(1)–F(1) 1.970(2), Ti(1)–F(2A) 2.059(2), Ti(1)–F(3) 1.967(2), Ti(1)···Ti(2A) 3.2162(10), Ti(2)–O(4) 1.801(3), Ti(2)–O(5) 1.980(3), Ti(2)–O(6) 1.785(3), Ti(2)–F(1A) 2.052(2), Ti(2)–F(2) 1.968(2), Ti(2)–F(3) 1.940(2); Ti(1)–F(1)–Ti(2A) 106.18(10), Ti(1)–F(3)–Ti(2) 176.22(13). Symmetry operator: $A = -x + 1, y, -z + \frac{1}{2}$.

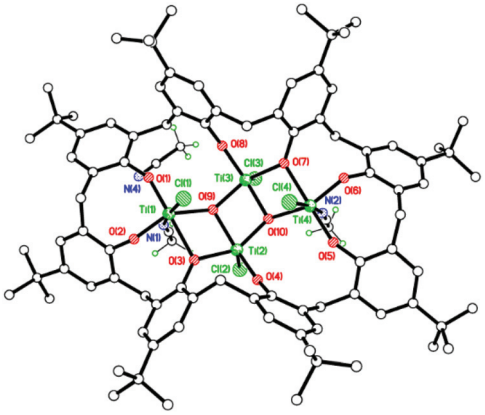

Fig. 3 Molecular structure of $[(TiCl)_2(TiClNCMe)_2(\mu_3\text{-}O)_2(L^2)]\cdot 1.5MeCN$ (**4**·1.5MeCN). Most H atoms, minor components of disordered atoms, and some solvent of crystallisation omitted for clarity. Selected bond lengths (Å) and angles (°): Ti(1)–O(1) 1.786(5), Ti(1)–O(2) 1.806(4), Ti(1)–O(3) 2.202(5), Ti(1)–O(9) 1.976(5), Ti(1)–Cl(1) 2.303(2), Ti(1)–N(1) 2.197(7), Ti(2)–O(3) 1.934(5), Ti(2)–O(4) 1.782(5), Ti(2)–O(9) 1.992(5), Ti(2)–O(10) 1.864(5), Ti(2)–Cl(2) 2.238(2); Cl(1)–Ti(1)–O(2) 102.65(17), O(1)–Ti(1)–O(9) 107.6(2), O(3)–Ti(2)–O(4) 95.3(2), Cl(2)–Ti(2)–O(3) 107.89(16), Cl(1)–Ti(1)–N(1) 171.11(18).

H-bonds. The central core can be described as two Ti_2F_2 diamonds, which bridge the calixarenes, whilst two fluoride ions bridge the two diamonds. The Ti–F bonds are somewhat longer than those found in the [O, N_{Py}, N]-bearing Ti complexes recently reported by Solan *et al.*[18] The MeCNs containing N(1) and N(2) reside in the calixarene cavity.

Use of *p-tert*-butylcalix[8]areneH$_8$ L^{2}H$_8$

Use of [TiCl$_4$]. Reaction of *p-tert*-butylcalix[8]areneH$_8$ (L^2H_8) with [$TiCl_4$] (four equivalents) in refluxing toluene affords, following work-up (extraction into MeCN), small red crystals in moderate yield. A single crystal X-ray diffraction study revealed the complex to be the laddered species $[(TiCl)_2(TiClNCMe)_2(\mu_3\text{-}O)_2(L^2)]\cdot 1.5MeCN$ (**4**·1.5MeCN) (CCDC 1973133†), and this formula represents the asymmetric unit, see Fig. 3. The Ti(1) and Ti(4) centres are pseudo-octahedral with *trans* Cl and MeCN ligands, whilst Ti(2) & Ti(3) are square-based pyramidal with apical Cl ligands. The result is a central Ti_4O_4 ladder, which is supported by the fully deprotonated saddle-shaped L^2 ligand. Such ladders have been observed previously in *p-tert*-butylcalix[4 and 6]arene titanium chemistry.[19] The Cl ligands on the two central Ti centres both point the same way, while those on the terminal Ti centres point the opposite way (see ESI, Fig. S5†). We have recently reported the same complex, however on that occasion it could only be isolated as a co-crystallized mixture (35 : 65) with a silicone grease derived complex $[Ti(NCMe)Cl]_2[Ti(\mu\text{-}O)]_2[OSi(CH_3)_2OSi(CH_3)_2O]L^2]$ in which the grease replaces two chloride ligands.[20]

Some weak C–H···Cl intermolecular interactions parallel to *a* bind molecules into anti-parallel stacks (see ESI, Fig. S6†). In one preparation of **4**, following work-up and crystallization from MeCN, the isolated crystals were identified as $[Ti_4O_2Cl_4(MeCN)_2(L^2)][Ti_3Cl_6(MeCN)_5(OH_2)(L^2H_2)][OH_2]\cdot 11MeCN$ (**5**·11MeCN; CCDC 1973135†). The asymmetric unit of **5** contains 2 different molecules (Fig. 4). In one molecule there is a ladder structure, like **4**, made up of four Ti(IV) ions and phenolate oxygens (from the L^2 ligand) and bridging oxygens, O(3), O(7), O(9), and O(10). The latter two are oxo dianions. Ti(1) and Ti(4) each carry 1 Cl^- ion and one MeCN ligand; Ti(2) and Ti(3) each carry one Cl^- ion. In the other molecule, three Ti(IV) ions are coordinated to a L^2H_2 ligand *via* 6 phenolate oxygens (two per Ti); and oxygens O(17) and O(18) remain protonated. Ti(5) and Ti(6) are each coordinated to two Cl^- ions and two MeCN ligands, and Ti(7) is coordinated to two Cl^- ions, one MeCN ligand and one water molecule. There are two intramolecular H-bonds: O(18)–H(18)···O(17) and O(17)–H(17)···Cl(9), and a lone water molecule sits between the two titanium-calixarene molecules. The H atoms could not be located for this or the coordinated water molecule, but both appear to form reasonable H-bonds: O(19)···N(5) = 2.681, O(19)···O(20) = 2.759, and O(20)···Cl(1) = 3.525 Å. In terms of intermolecular interactions between molecules, the water molecule between the two different calix[8]arene complexes hydrogen bonds to the coordinated water molecule. The coordinated water molecule H-bonds to an acetonitrile molecule of crystallization.

Use of [TiBr$_4$]. Similar use of [$TiBr_4$] with L^2H_8 led to a very similar ladder complex (see Fig. 5), with crystallization from MeCN affording $[(TiBr)_2(TiBrNCMe)_2(\mu_3\text{-}O)_2(L^2)]\cdot 6MeCN$ (**6**·6MeCN), which is the asymmetric unit (CCDC 1973132†).

Both coordinated MeCN groups point to the same side of the molecule, whilst the six MeCN molecules of crystallization are all *exo* to the complex. Molecules pack in layers. Adjacent

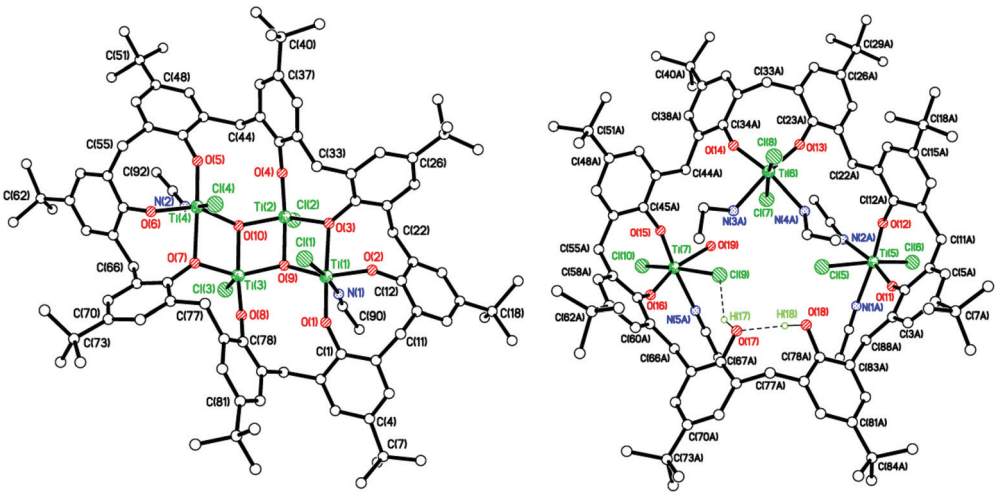

Fig. 4 Molecular structures of the two Ti complexes co-crystallised in $[Ti_4O_2Cl_4(MeCN)_2(L^2)][Ti_3Cl_6(MeCN)_5(OH_2)(L^2H_2)][OH_2]\cdot 11MeCN$ (**5**·11MeCN). Solvent of crystallization, minor components of disordered atoms, and most H atoms omitted for clarity. Selected bond lengths (Å) and angles (°): Ti(1)–O(1) 1.798(3), Ti(1)–O(2) 1.796(3), Ti(1)–O(3) 2.185(3), Ti(1)–O(9) 1.958(3), Ti(1)–Cl(1) 2.3109(17), Ti(1)–N(1) 2.269(5), Ti(2)–O(3) 1.944(3), Ti(2)–O(4) 1.769(3), Ti(2)–O(9) 1.995(3), Ti(2)–O(10) 1.896(3), Ti(2)–Cl(2) 2.133(3), Ti(5)–O(11) 1.780(3), Ti(5)–O(12) 1.769(3), Ti(5)–Cl(5) 2.3707(19), Ti(5)–Cl(6) 2.3331(17), Ti(5)–N(1A) 2.233(4), Ti(5)–N(2A) 2.205(4), Ti(6)–O(13) 1.785(4), Ti(6)–O(14) 1.815(3), Ti(6)–Cl(7) 2.3904(17), Ti(6)–Cl(8) 2.3229(19), Ti(6)–N(3A) 2.165(4), Ti(6)–N(4A) 2.158(4), Ti(7)–O(15) 1.776(3), Ti(7)–O(16) 1.803(3), Ti(7)–O(19) 2.104(4), Ti(7)–Cl(9) 2.4734(15), Ti(7)–Cl(10) 2.3155(16), Ti(7)–N(5A) 2.237(4); Cl(1)–Ti(1)–O(2) 102.51(12), O(1)–Ti(1)–O(9) 107.79(14), Cl(1)–Ti(1)–N(1) 172.39(10), O(3)–Ti(2)–O(4) 95.74(13), Cl(2)–Ti(2)–O(3) 105.99(12), Cl(5)–Ti(5)–Cl(6) 162.91(7), O(11)–Ti(5)–N(1A) 88.65(15), O(12)–Ti(5)–N(2A) 88.58(16), Cl(7)–Ti(6)–Cl(8) 165.98(7), O(13)–Ti(6)–N(3A) 173.17(16), O(14)–Ti(6)–N(4A) 169.60(16), Cl(9)–Ti(7)–Cl(10) 167.29(6), O(15)–Ti(7)–N(5A) 173.91(15), O(16)–Ti(7)–O(19) 164.48(15).

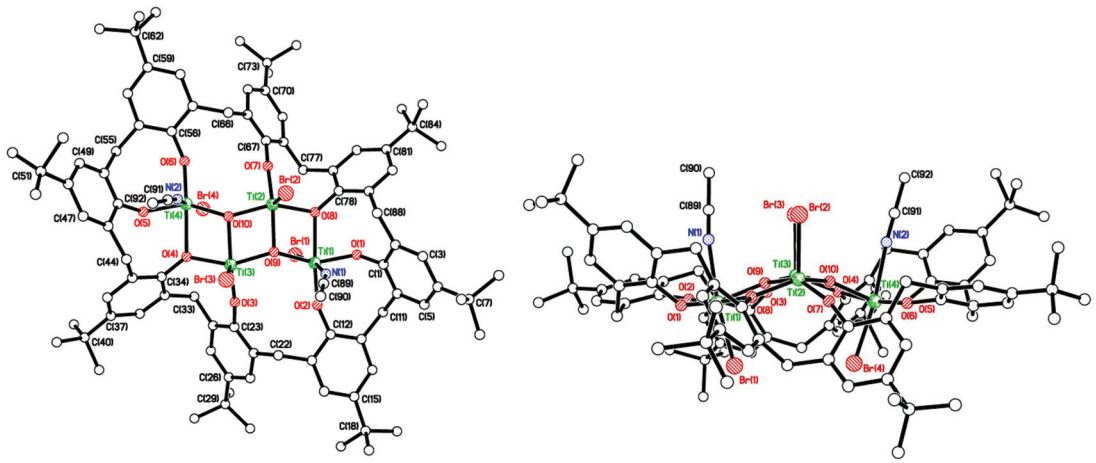

Fig. 5 Two views of the molecular structure of $[(TiBr)_2(TiBrNCMe)_2(\mu_3\text{-}O)_2(L^2)]\cdot 6MeCN$ (**6**·6MeCN). MeCN of crystallization, minor components of disordered atoms, and H atoms omitted for clarity. Selected bond lengths (Å) and angles (°): Ti(1)–O(1) 1.8153(15), Ti(1)–O(2) 1.7834(16), Ti(1)–O(8) 2.1529(15), Ti(1)–O(9) 1.9668(16), Ti(1)–Br(1) 2.4484(5), Ti(1)–N(1) 2.327(2), Ti(2)–O(8) 1.9490(15), Ti(2)–O(7) 1.7620(15), Ti(2)–O(9) 1.9819(16), Ti(2)–O(10) 1.8859(15), Ti(2)–Br(2) 2.3871(4); Ti(1)–O(1)–C(1) 131.18(14), Ti(1)–O(2)–C(12) 158.93(14), Ti(1)–O(8)–C(78) 126.59(12), Ti(2)–O(7)–C(67) 166.45(15), Ti(1)–O(8)–Ti(2) 103.12(6), Ti(1)–O(9)–Ti(3) 146.33(9), O(8)–Ti(2)–O(10) 146.05(7.

molecules within layers adopt up–down–up–down orientations (see Fig. S7, ESI†). Between layers molecules stack in columns all pointing in the same direction with weak Br(1)···Br(2′) = 3.770 Å halogen bonding interactions. Given the addition of differing amounts of metal chloride to a calix[*n*]arene can be used to control the degree of metalation,[8] we also investigated the addition of three equivalents of $[TiBr_4]$. This resulted, following work-up (MeCN), in the formation of brown prisms for which a molecular structure determination revealed the asymmetric unit $\{[TiBr_2(H_2O)(NCMe)][TiBr_2(NCMe)_2Ti]_2L^2H_2\}\cdot 7.5(MeCN)$ 7·7.5(MeCN), see Fig. 6 (CCDC 1973131†). The calix[8]arene ligand retains two phenolic hydrogens on oxygens O(7) and O(8), which are not bound to titanium ions. Three $TiBr_2$ moieties bind to the L^2H_2 *via* two phenolate oxygens each. Each Ti ion has octahedral geometry. The bromides are *trans* on Ti(1) and Ti(2), but *cis* on Ti(3).

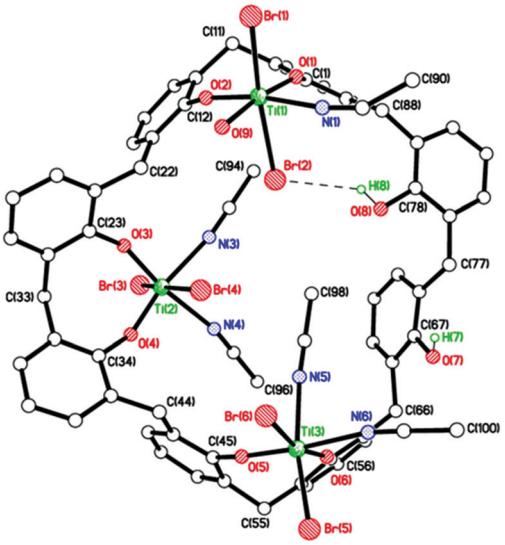

Fig. 6 Molecular structure of $[[Ti(NCMe)_2Br]_2[Ti(O)Br_2(NCMe)](L^2)]\cdot 7.5MeCN$ (**7**·7.5MeCN). Calixarene ^{t}Bu groups, minor components of disordered atoms, and MeCN of crystallization omitted for clarity. Selected bond lengths (Å) and angles (°): Ti(1)–O(1) 1.793(5), Ti(1)–O(2) 1.796(5), Ti(1)–O(9) 2.154(6), Ti(1)–Br(1) 2.5066(15), Ti(1)–Br(2) 2.5496(14), Ti(1)–N(1) 2.193(7), Ti(2)–O(3) 1.785(4), Ti(2)–O(4) 1.777(5), Ti(2)–Br(3) 2.5224(16), Ti(2)–Br(4) 2.5375(16), Ti(2)–N(3) 2.206(5), Ti(2)–N(4) 2.228(6), Ti(3)–O(5) 1.774(4), Ti(3)–O(6) 1.808(5), Ti(3)–Br(5) 2.4653(13), Ti(3)–Br(6) 2.5371(15), Ti(3)–N(5) 2.188(5), Ti(3)–N(6) 2.260(7); Ti(1)–O(1)–C(1) 146.1(4), Ti(1)–O(2)–C(12) 150.3(4), Br(1)–Ti(1)–Br(2) 166.29(7), O(1)–Ti(1)–O(9) 170.4(2), Ti(2)–O(3)–C(23) 151.1(4), Ti(2)–O(4)–C(34) 150.7(4), Br(3)–Ti(2)–Br(4) 169.37(6), Ti(3)–O(5)–C(45) 152.4(4), Ti(3)–O(6)–C(56) 155.5(4), Br(5)–Ti(3)–Br(6) 94.43(5).

The remaining coordination sites are occupied by MeCN ligands in the case of Ti(2) and Ti(3), while Ti(1) bears one MeCN and most likely a water molecule. No peaks corresponding to carbon atoms were evident close to that water molecule that would have indicated MeCN. There is one intramolecular hydrogen bond between one of the phenol groups and one of the coordinated bromide ions. The other phenolic hydrogen does not make a hydrogen bond. Molecules are arranged in an undulating layer structure in the *a*/*c* plane (see Fig. S8,† ESI).

Use of $[TiF_4]$. Use of $[TiF_4]$ and L^2H_8 led, following work-up in MeCN, to more complicated species in which both sodium and calcium have been incorporated. The presence of these alkali/alkaline earth metals is thought to arise from the predrying of the solvents, namely toluene and acetonitrile respectively. The small red prisms obtained were subjected to an X-ray diffraction study (CCDC 1973130†), and two views of the molecular structure of **8** are given in Fig. 7 (an alternative view is given in the ESI, Fig. S9†); selected bond lengths and angles are given in the caption. The complex has the formula $[Ti_8CaF_{20}(OH_2)Na_2(MeCN)_4(L^2)_2]\cdot 14MeCN$ (**8**·14MeCN), and lies on a mirror plane, which includes atoms Ca(1), Na(1), Na(2), some of the fluoride ions and the water molecule. The main core of the molecule comprises 8 titanium ions and 20 fluoride ions (a mixture of terminal and bridging), see Fig. 7. Each titanium ion binds to a L^2 ligand *via* two phenolate oxygens, and each L^2 binds to four octahedral titanium ions. The oxygens bound to each individual titanium atom are *cis*. A calcium ion and two sodium ions are present to balance out the overall charge. The part of the core of the molecule containing the Ca^{2+} ion is antifluorite-like with the Ca^{2+} coordinated by 9 F ions. Na(1) interacts with fluorides F(6) and

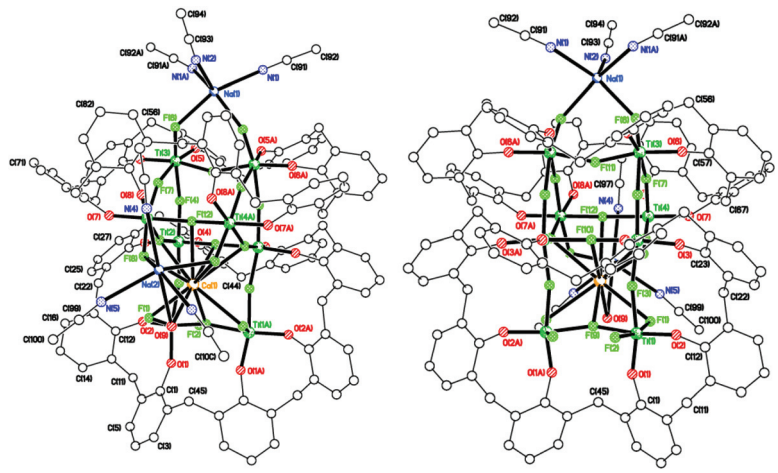

Fig. 7 Two views of the molecular structure of $[Ti_8CaF_{20}(OH_2)[Na_2(MeCN)_4](L^2)_2]\cdot 14MeCN$ (**8**·14MeCN). MeCN of crystallization, calixarene ^{t}Bu groups, minor components of disordered atoms, and H atoms omitted for clarity. Selected bond lengths (Å) and angles (°): Ti(1)–O(1) 1.757(7), Ti(1)–O(2) 1.790(6), Ti(1)–F(1) 1.903(7), Ti(1)–F(2) 1.957(6), Ti(1)–F(3) 2.009(4), Ti(1)–F(9) 2.010(3), Ti(2)–O(3) 1.775(4), Ti(2)–O(4) 1.760(6), Ti(2)–F(3) 1.938(4), Ti(2)–F(4) 1.907(4), Ti(2)–F(5) 2.020(4), Ti(2)–F(10) 2.0063(14), Ti(3)–O(5) 1.802(5), Ti(3)–O(6) 1.796(4), Ti(3)–F(4) 2.012(5), Ti(3)–F(6) 1.806(5), Ti(3)–F(7) 1.983(4), Ti(3)–F(11) 1.9688(15), Ti(4)–O(7) 1.797(4), Ti(4)–O(8) 1.782(6), Ti(4)–F(5) 2.036(5), Ti(4)–F(7) 1.956(4), Ti(4)–F(8) 1.839(4), Ti(4)–F(12) 2.0104(16), Ca(1)–F(1) 2.889(6), Ca(1)–F(5) 2.869(4), Ca(1)–F(8) 2.716(5), Ca(1)–F(9) 2.776(11), Ca(1)–F(10) 3.027(5), Ca(1)–F(12) 2.858(7); Ti(1)–F(9)–Ti(1A) 146.0(4), Ti(1)–F(3)–Ti(2) 168.1(2), Ti(2)–F(10)–Ti(2A) 160.7(3), Ti(2)–F(5)–Ti(4) 152.3(2), Na(2)–O(9)–Ca(1) 85.8(4).

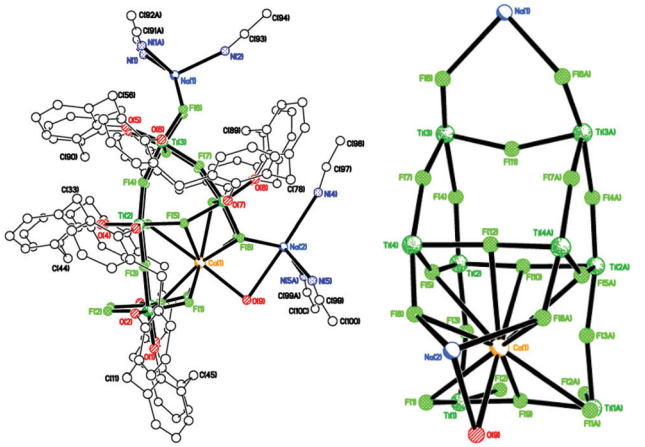

Fig. 8 Side view (left) and core of the structure (right) of $[Ti_8CaF_{20}(OH_2)(Na_2(MeCN)_4)(L^2)_2]\cdot 14MeCN$ (**8**·14MeCN).

F(6A), and three acetonitrile molecules: *via* N(1), N(1A), and N(2). Na(2) interacts with fluorides F(8) and F(8A), water molecule O(9), and three acetonitrile molecules: containing N(4), N(5), and N(5A). The H atoms on the water molecule could not be located from difference maps. The water molecule bridges the calcium ion and one of the sodium ions. Four of the calixarene rings of each separate calixarene, bound to O atoms O(3), O(3A), O(4), and O(4A) on one, and O(5), O(5A), O(6), and O(6A) on the other, are close in space and adopt the same conformation, stacking almost exactly on top of each other, see Fig. 8 and S9, ESI.† The titanocalix[8]arene molecules are generally well separated, with no significant intermolecular interactions between them. Viewed perpendicular to *b*/*c* plane, it can be seen that there are significant solvent filled voids in the structure (Platon Squeeze recovers 291 electrons in 2 voids, giving 14 MeCNs per unit cell or an extra 7 MeCNs per Ti_8 complex), see Fig. S10, ESI.† [21]

We note that Ti–F complexes in which alkaline or alkaline-earth metal ions are featured in the structure in a host–guest fashion have been previously reported.[22] However, these species were intentionally synthesized in a template-controlled manner, while the Na^+ and Ca^{2+} ions present in **8** are likely to derive from the drying agents of the solvents used for the reaction/workup and are serendipitously incorporated into the structure.

To investigate the reproducibility of such species, we repeated the reaction (using the same batch of L^2H_8) and again isolated red prisms. However, on this occasion the asymmetric unit (CCDC 1973365†) was found to be $[Na(MeCN)_2][Ti_8CaF_{20}NaO_{16}(L^2)_2]\cdot 7MeCN$ (**9**·7MeCN), see Fig. 9, and unlike **8**·14MeCN, it is not on a mirror plane, *i.e.* the whole molecule is unique, although there are also many similarities. The main core of the molecule again comprises 8 titanium ions and 20 fluoride ions with the fluorides a mixture of terminal and bridging Ti(3) and Ti(4) have 4 bridging fluorides, and Ti(5) > Ti(8) have 1 terminal and 3 bridging fluorides. Each octahedral titanium ion binds

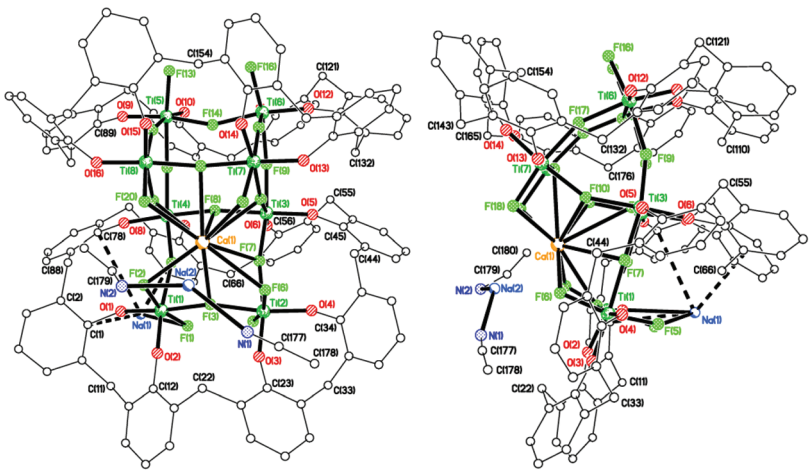

Fig. 9 Two almost perpendicular views of the molecular structure of $[Na(MeCN)_2][Ti_8CaF_{20}NaO_{16}(L^2)_2]\cdot 7MeCN$ (**9**·7MeCN). MeCN of crystallization, calixarene tBu groups, minor components of disordered atoms, and H atoms omitted for clarity. Selected bond lengths (Å) and angles (°): Ti(1)–O(1) 1.812(4), Ti(1)–O(2) 1.769(5), Ti(1)–F(1) 2.014(5), Ti(1)–F(2) 1.895(4), Ti(1)–F(3) 2.013(3), Ti(1)–F(4) 2.028(4), Ti(2)–O(3) 1.785(5), Ti(2)–O(4) 1.831(4), Ti(2)–F(3) 2.033(3), Ti(2)–F(5) 1.938(4), Ti(2)–F(6) 1.892(4), Ti(2)–F(7) 2.033(4), Ti(3)–O(5) 1.778(4), Ti(3)–O(6) 1.763(4), Ti(3)–F(7) 1.961(4), Ti(3)–F(8) 2.002(3), Ti(3)–F(9) 1.927(3), Ti(3)–F(10) 2.003(3), Ti(4)–O(7) 1.791(5), Ti(4)–O(8) 1.779(4), Ti(4)–F(4) 1.949(4), Ti(4)–F(8) 2.002(3), Ti(4)–F(11) 1.919(4), Ti(4)–F(12) 2.038(4), Ti(5)–O(9) 1.788(4), Ti(5)–O(10) 1.807(5), Ti(5)–F(11) 2.021(4), Ti(5)–F(13) 1.829(4), Ti(5)–F(14) 1.963(3), Ti(5)–F(15) 2.009(4), Ti(6)–O(11) 1.793(5), Ti(6)–O(12) 1.786(4), Ti(6)–F(9) 2.027(3), Ti(6)–F(14) 1.973(3), Ti(6)–F(16) 1.829(4), Ti(6)–F(17) 1.981(4), Ti(7)–O(13) 1.818(4), Ti(7)–O(14) 1.777(5), Ti(7)–F(10) 2.009(3), Ti(7)–F(17) 1.696(4), Ti(7)–F(18) 1.856(4), Ti(7)–F(19) 2.054(3), Ti(8)–O(15) 1.795(5), Ti(8)–O(16) 1.838(4), Ti(8)–F(12) 2.051(4), Ti(8)–F(15) 1.950(4), Ti(8)–F(19) 2.025(3), Ti(8)–F(20) 1.857(4), Ca(1)–F(2) 2.736(4), Ca(1)–F(3) 2.669(4), Ca(1)–F(6) 2.888(4), Ca(1)–F(7) 3.073(4), Ca(1)–F(8) 3.068(4), Ca(1)–F(10) 2.807(3), Ca(1)–F(12) 2.901(4), Ca(1)–F(18) 2.675(4), Ca(1)–F(19) 2.809(4), Ca(1)–F(20) 2.773(4); Ti(1)–F(3)–Ti(2) 152.3(2), Ti(1)–F(4)–Ti(4) 162.68(19), Ti(2)–F(7)–Ti(3) 167.34(18), Ti(3)–F(8)–Ti(4) 159.17(19), F(2)–Ca(1)–F(10) 153.10(13), F(3)–Ca(1)–F(19) 150.59(13).

to an L^2 ligand *via* two phenolate oxygens; each L^2 binds to 4 titanium atoms. The oxygens bound to each individual titanium atom are *cis*. A calcium ion and two sodium ions are present to balance out the overall charge. The part of the core of the molecule containing the Ca^{2+} ion (see Fig. 10) is anti-fluorite-like with the Ca^{2+} coordinated by 11 F^- ions, rather than the 9 in **8**. Na(1) interacts with fluoride F(1), phenolate oxygen O(1), two *ipso* phenolate carbons C(1) and C(78), and the π-system of phenolate ring C(67) > C(72). Na(2) binds to two acetonitrile molecules, *via* N(1) and N(2), as a separate moiety in fairly close proximity to the Ca^{2+} ion and its co-ordinated fluorides.

Again, as in **8**, four of the calixarene rings of each separate calixarene, bound to O atoms O(5) > O(8) on one, and O(9) > O(12) on the other, are close in space and adopt the same conformation, stacking almost exactly on top of each other. MeCN molecules and MeCN-solvated Na^+ ions lie between titanocalix[8]arene complexes.

The complex $[Na]_6[Ti_8F_{20}Na(MeCN)_2(L^2)]$-$[Ti_8F_{20}Na(MeCN)_{0.5}(L^2)]\cdot 15.5(C_2H_3N)$ (**10**·15.5MeCN) has also been isolated and structurally characterized (see Fig. 11) from a re-run of this type of reaction, indicating that the products formed are variable and their exact nature is determined by the presence of drying agents in the solvents. For **10**, there are negative charges: 2 × calix[8] = 16−, 20 × F^- = 20−, total 36−; positive charges: 8 × Ti^{4+} = 32+, and 1 × Na^+ gives a total of 33+. It is assumed that there are also another 3 Na^+ ions to balance the charge and these are modelled by the Platon Squeeze procedure due to disorder and being randomly distributed between the MeCN molecules of crystallization.[21] The amount of MeCN of crystallization should be regarded as approximate. There are two almost identical molecules in the asymmetric unit, differing only in the coordination site of the sodium ion and the number of acetonitrile molecules bonded to the sodium. The main core of each molecule is made up of 8 titanium ions and 20 fluorides as seen previously in **8** and **9** (see Fig. 12, and Fig. S11, ESI†). Two titanium ions have 2 terminal fluorides and 2 bridging fluorides, four titanium ions have 1 terminal fluoride and 3 bridging fluorides, and the remaining two titanium ions have 4 bridging fluorides. Each titanium ion binds to a L^2 ligand *via* two phenolate oxygens; and each L^2 binds to 4 titanium ions. Each Ti ion has octahedral geometry. The oxygens bound to each individual titanium atom are *cis*. In the first molecule, sodium ion Na(1) interacts with fluoride F(6) and two acetonitrile molecules including N(5) and N(9). In the second molecule, the major occupancy site of disordered sodium ion Na(2) interacts with fluorides F(25) and F(28), and the acetonitrile molecule including N(11), which was refined at half occupancy to match that of the major Na(2) component. Each pair of calixarene rings, on each titanium–fluoride core, are close in space and adopt the same conformation, stacking almost exactly on top of each other as seen previously (see Fig. 12 and S12, ESI†). MeCN molecules lie between titanocalixarene complexes. Also in this case, the Ti–F bonds for complexes **8–10** are slightly longer than those observed in previously reported compounds.[18]

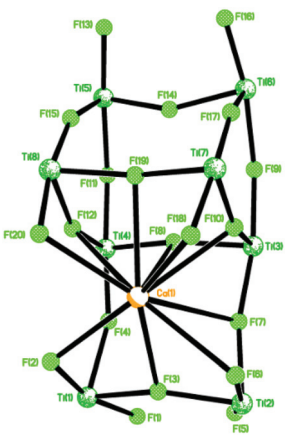

Fig. 10 Core of the structure of $[Na(MeCN)_2][Ti_8CaF_{20}NaO_{16}(L^2)_2]\cdot 7MeCN$ (**9**·7MeCN).

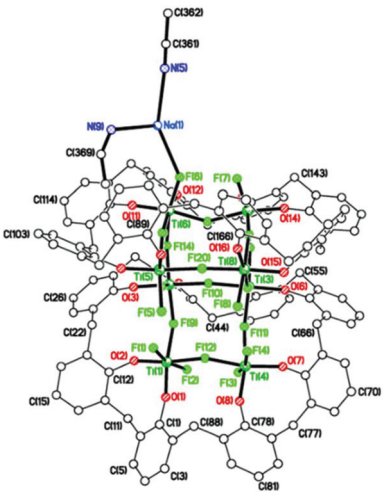

Fig. 11 The molecular structure of one of the two unique molecules in $[Na]_6[Ti_8F_{20}Na(MeCN)_2(L^2)]$-$[Ti_8F_{20}Na(MeCN)_{0.5}(L^2)]\cdot 15.5(C_2H_3N)$ (**10**·15.5MeCN). Calixarene ^{t}Bu groups, minor components of disordered atoms, MeCN of crystallization, and H atoms omitted for clarity. Selected bond lengths (Å) and angles (°): Ti(1)–F(1) 1.905(4), Ti(1)–F(2) 2.079(4), Ti(1)–F(9) 1.991(3), Ti(1)–F(12) 1.980(3), Ti(2)–F(9) 1.924(3), Ti(3)–F(10) 1.994(3), Ti(3)–F(11) 1.950(3), Ti(6)–F(6) 2.020(4), Na(1)–F(6) 2.696(4); Ti(1)–F(9)–Ti(2) 157.05(18), Ti(1)–F(12)–Ti(4) 149.4(2), Ti(3)–F(10)–Ti(12) 160.26(17), Ti(3)–F(11)–Ti(4) 165.40(17), Ti(5)–F(20)–Ti(8) 160.75(18).

Use of [TiI_4]. Treatment of L^2H_8 with four equivalents of [TiI_4] in toluene afforded, following work-up in dichloromethane, a dark red complex which was isolated as large blocks. Interestingly, the molecular structure revealed (see Fig. 13) a ladder complex similar to that observed for the chloride and bromide systems. The asymmetric unit comprises $[Ti_4I_4O_2(MeCN)_2(L^2)]\cdot 7.25(CH_2Cl_2)$ (**11**·7.25CH_2Cl_2; CCDC 1973364†). There are CH_2Cl_2 molecules both in calixarene clefts and *exo* to the calix[8]arene. There are some C–H···π interactions involving CH_2Cl_2 to calixarene rings. The molecules form layers in the *a*/*c* plane (see Fig. S13, ESI†).

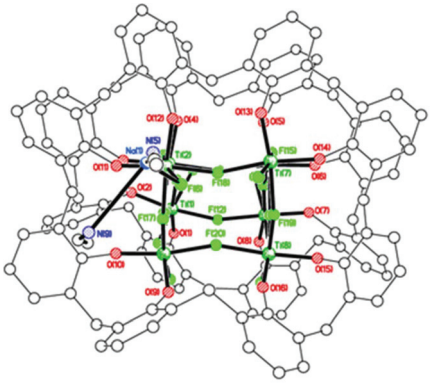

Fig. 12 Diagram of **10**, emphasizing the core connectivity and partial calixarene overlay. Calixarene ^{t}Bu groups, MeCN of crystallization, and H atoms omitted for clarity.

Table 1 summarises the Ti–X bond length data from the four ladder structures described above. There are two main observations. Firstly, the Ti–X bond length increases by approx. 0.2 Å on going from Cl to Br and from Br to I, in line with the ionic radius increases as Group 17 is descended. Secondly, the Ti–X bond lengths for the halide attached to the six-coordinate end Ti ions, and *trans* to an MeCN nitrogen, is significantly longer (by 0.07–0.12 Å) than those for the apical halide attached to the central, five-coordinate, Ti ions with approx. square-based pyramidal geometry.

For catalysis comparison purposes, we have synthesised two diphenolate complexes bearing Br and I labile ligands, namely **12** and **13** (Scheme 1).

For the bromo-derivative **12**, crystals suitable for X-ray analysis were obtained at room temperature from a saturated solution of the compound in hexane. The molecular structure of the complex (CCDC 2009076†) is shown in Fig. 14. The compound features a tetrahedral Ti^{4+} ion. The complex molecule and the hexane of crystallization both lie on a mirror plane, so half of the formula is unique. The dihedral angle between aromatic rings was found to be 64°. The hexane molecule lies in the cleft between the two aromatic rings. There is a weak intermolecular C–H···Br interaction between the methyl group at C(16) and Br(1) with an H(16A)···Br(1) distance of 3.05 Å.

ROP screening

ε-Caprolactone (ε-CL). We have examined the ability of the complexes prepared herein (not **2**, **5**, **7**, and **8**) to act as cata-

Table 1 Summary of Ti–X bond lengths in ^{t}BuCalix[8]arene ladder structures

Structure	X	Av. Ti–X for X on central Ti/Å	Av. Ti–X for X on end Ti/Å	Difference, Δ/Å
4 & **5**	Cl	2.173(2)	2.297(2)	0.124
6	Br	2.381(4)	2.448(5)	0.067
11	I	2.592(2)	2.682(2)	0.090

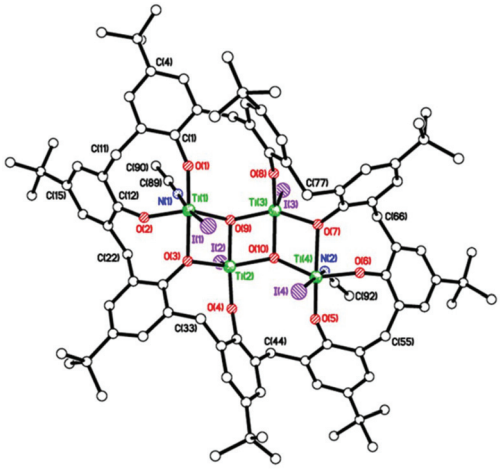

Fig. 13 Molecular structure of $[Ti_4I_4O_2(MeCN)_2(L^2)]\cdot 7.25(CH_2Cl_2)$ (**11**·7.25CH_2Cl_2). CH_2Cl_2 of crystallization, minor components of disordered atoms, and H atoms omitted for clarity. Selected bond lengths (Å) and angles (°): Ti(1)–O(1) 1.792(7), Ti(1)–O(2) 1.825(6), Ti(1)–O(3) 2.165(6), Ti(1)–O(9) 1.959(7), Ti(1)–I(1) 2.676(2), Ti(1)–N(1) 2.274(11), Ti(2)–O(3) 1.940(6), Ti(2)–O(4) 1.754(6), Ti(2)–O(9) 2.009(7), Ti(2)–O(10) 1.898(6), Ti(2)–I(2) 2.5935(18); I(1)–Ti(1)–O(2) 100.5(2), O(1)–Ti(1)–O(9) 106.7(3), I(1)–Ti(1)–N(1) 173.7(2), O(3)–Ti(2)–O(4) 95.6(3), I(2)–Ti(2)–O(3) 108.1(2).

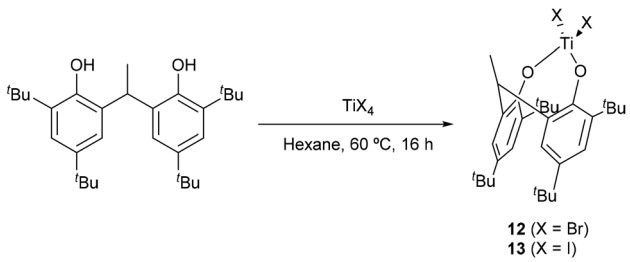

Scheme 1 Synthesis of the diphenolate complexes **12** and **13**.[14]

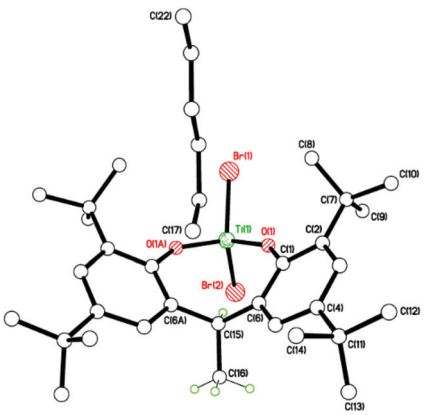

Fig. 14 Molecular structure of $[TiBr_2(diphenolate)]\cdot$hexane (**12**·hexane). Most H atoms and minor components of disordered atoms omitted for clarity. Selected bond lengths (Å) and angles (°): Ti(1)–O(1) 1.7597(18), Ti(1)–Br(1) 2.3796(7), Ti(1)–Br(2) 2.3810(7), O(1)–Ti(1)–Br(1) 110.55(6), Br(1)–Ti(1)–Br(2) 109.14(3), O(1)–Ti(1)–O(1A) 104.85(12), O(1A)–Ti(1)–Br(1) 110.85(7). Symmetry operator *A* = –*x* + 1, *y*, *z*.

Table 2 ROP of ε-CL using complexes **1**, **3**, **4**, **6**, **9** and **11–13**

Run	Catalyst	ε-CL : Ti : BnOH	T (°C)	Time (h)	Conv.[a] (%)	M_n[b,c]	$M_{n\ calc}$[d]	M_w/M_n[b]
1	**1**	500 : 1 : 3	80	24	None	—	—	—
2		250 : 1 : 3	130	24	69	5240	6700	1.22
3		250 : 1 : 3	130	1	6.5	—	—	—
4[e]		500 : 1 : 3	130	24	20	2690	3860	1.20
5[e]		500 : 1 : 3	130	1	None	—	—	—
6	**3**	250 : 1 : 4	130	24	None	—	—	—
7	**4**	500 : 1 : 2	80	24	None	—	—	—
8		250 : 1 : 1	130	24	8.4	—	—	—
9		250 : 1 : 1	130	1	None	—	—	—
10	**6**	500 : 1 : 2	80	24	None	—	—	—
11		250 : 1 : 1	130	24	None	—	—	—
12		250 : 1 : 1	130	1	None	—	—	—
13	**9**	250 : 1 : 1	130	24	64	8590	18 230	1.63
14		250 : 1 : 1	130	1	None			
15	**11**	250 : 1 : 1	130	24	74	6610	21 110	1.23
16		250 : 1 : 1	130	1	None			
17	**12**	250 : 1 : 2	80	24	>99	6720	14 210	1.40
18[e]		250 : 1 : 2	130	24	>99	5790	14 210	1.94
19	**13**	250 : 1 : 2	80	24	42	Liquid oligomers		
20		250 : 1 : 2	130	24	>99	5640	14 210	1.30

[a] Determined by ^{1}H NMR spectroscopy on crude reaction mixture. [b] From GPC. [c] Values corrected considering Mark–Houwink factor (0.56) from polystyrene standards in THF. [d] Calculated from ($[Monomer]_0/[OH]_0$) × conv. (%) × Monomer molecular weight + Molecular weight of BnOH. [e] Reaction performed in air.

lysts for the ROP of ε-CL (Table 2). At 80 °C, **1**, **4** and **6** were found to be inactive (runs 1, 7, and 10). By increasing the temperature to 130 °C, 69% conversion was achieved in the presence of **1** in 24 h, while low activity was observed after 1 h (runs 3 and 5). Interestingly, the complex proved to be active also under aerobic conditions achieving *ca.* 20% conversion during 24 h (run 4). The M_n of the isolated polymers were found to be lower than the calculated values, while narrow polydispersities (1.20) were observed. Complex **3** was found to be inactive (run 6). Amongst the larger titanocalix[8]arene complexes, moderate conversion of the monomer was achieved only in the presence of **9** and with its iodo-congener **11** (63 and 74%, runs 13 and 15 respectively), while both chloro- and bromo-derivatives were found to be inactive. The higher activity of **1** compared with that of **4** and **6** can be explained considering the lability of the ligands present. In fact, the Ti ions in **1** are bound either to MeCN or H_2O, which are more readily lost than the halides in **4** and **6**. Similarly, the lability of the iodo-ligands would be responsible for the higher activity of **11** compared to that of its Cl- and Br-containing analogues. This is in line with our recent study on titanocalix[4]arenes, in which the presence of a labile ligand (*i.e.* MeCN) proved beneficial for the catalyst activity.[14] In addition, the arrangement of and distance between the two Ti centers in **1** could favour cooperative effects enhancing the catalytic performances. On the other hand, this might not be possible for **4**, **6**, and **11** in which the metals are connected in a [Ti–O–Ti] fashion. Similar trends were observed in the case of multimetallic Al complexes bearing macrocyclic Schiff-bases, where both the distance and bond types present dictated the observed activity.[23] The efficiency of **9** is thought to be due to cooperative effects of the Ti and of Ca/Na cations present in the structure.

The bromo-(**12**) and iodo-(**13**) diphenolate titanium complexes were next investigated. Full conversion was achieved in the presence of the bromo derivative **12** at 80 °C within 24 h (run 17) affording a polymer with M_n of *ca.* 6.7 kDa and rather narrow polydispersity (1.40). Interestingly, complex **12** proved to be efficient also under aerobic conditions at 130 °C, but with less control (run 18). However, in both cases, the M_n were found to be much lower than the calculated values, suggesting the occurrence of transesterification processes. ^{1}H NMR spectroscopic analysis on the sample isolated in run 16 highlighted the presence of signals at 7.33, 5.09 and 3.64 ppm in an integration ratio of 5 : 2 : 2, compatible with the presence of both BnO– and CH_2OH end groups (Fig. S14, ESI†). This was further confimed by mass spectrometry. Indeed, the MALDI-ToF spectrum of the sample displayed a major series of peaks separated by 114 m/z units accountable to α-BnO-ω-OH terminated PCL *n*-mers as well as a minor population attributed to the corresponding Na^+ adducts (Fig. S15, ESI†). The iodo-congener **13** was shown to be less efficient, affording 40% conversion at 80 °C (run 19) and low molecular weight oligomers. Interestingly, full conversion was achieved on increas-

ing the temperature to 130 °C, affording a polymer of M_n 5.6 kDa with good control (M_w/M_n 1.30) (run 20). The higher activity of the diphenolate complexes can be ascribed to the increased accessibility of their metal centres compared with that of the calix[*n*]arene derivatives. However, **12** and **13** proved less active than related diphenolate species previously reported by Aida *et al.*[24]

δ-Valerolactone (δ-VL). Furthermore, the ROP of δ-valerolactone (δ-VL) was investigated (Table 3). Similar to the ε-CL case, **1** was found to be poorly active at 80 °C (runs 1 and 2). By increasing the temperature to 130 °C and lowering the monomer to catalyst ratio, moderate conversion was achieved in 24 h (run 3). For the isolated polymer, narrow polydispersity (1.13) and M_n higher than the calculated value were observed. No conversion was achieved by preforming the reaction in air (run 4). Also in this case, **3** and **4** were found to be inactive (runs 5–9) while poor activity was exhibited by its Br-congener (runs 10–13). Moderate activity was exhibited by **9** over 24 h, affording a polymer of M_n close to the calculated values and with good selectivity (run 14). No reaction was observed after 1 h (run 15). Interestingly, *ca.* 70% conversion was obtained in the presence of **11** over 24 h (run 16). The M_n value was higher than the expected value and good control was observed. In the case of the di-phenolate derivatives **12** and **13**, at 80 °C within 24 h, only 52 and 41% conversion was achieved in the presence of the Br- and I-complexes, respectively (runs 18 and 20). The improvement of the conversion was obtained on increasing the temperature to 130 °C (runs 19 and 21). In fact, 64 and 53% conversion was achieved with **12** and **13**, respectively.

In both cases, polymers with M_n lower than the calculated values were isolated; however, better control was exhibited by **13** compared with its bromo-congener (M_w/M_n 1.4 *vs.* 1.9).

***rac*-Lactide (*r*-LA).** The selected complexes were also employed as catalysts in the ROP of *r*-LA (Table 4). Good conversion was achieved in the presence of **1** (87%, run 1). The M_n of the polymer was lower than the calculated value albeit with narrow molecular weight distribution (8000 and 1.29, respectively). The syndiotactic bias (P_r) was determined by 2D *J*-resolved NMR spectroscopy (see Fig. S16, ESI†).[25] The observed value (0.51) suggested the formation of atactic PL. No reaction was observed when employing **3**, **4**, and the bromide complex **6**, regardless of the reaction conditions investigated (runs 3–11). Unlike the previous cases, **9** was found to be completely inactive (runs 12 and 13). Eventually, 8% conversion was obtained in the presence of **11** over 24 h (run 14). On conducting the reaction in the presence of the bromotitanium diphenolate complex **12**, complete monomer conversion was achieved, affording a polymer with M_n of *ca.* 5.0 kDa with narrow dispersity (run 16). On the other hand, the iodo-congener only allowed for 37% monomer conversion affording low molecular weight species.

ε-CL/δ-VL co-polymerization. The co-polymerization of ε-CL and δ-VL was next investigated (Table 5). Moderate conversion (68%) was achieved in the presence of **1** (run 1) affording a

Table 3 ROP of δ-valerolactone using complexes **1**, **3**, **4**, **6**, **9** and **11–13**

Run	Catalyst	δ-VL : Ti : BnOH	*T* (°C)	Time (h)	Conversion[a] (%)	M_n[b]	$M_{n\mathrm{calc}}$[c]	M_w/M_n[b]
1	**1**	500 : 1 : 3	80	24	18			
2		500 : 1 : 3	80	1	None			
3		250 : 1 : 3	130	24	45.8	6360	3930	1.13
4[d]		500 : 1 : 3	130	24	None			
5	**3**	250 : 1 : 4	130	24	None	—	—	—
6	**4**	500 : 1 : 2	80	24	None			
7		500 : 1 : 2	80	1	None			
8		250 : 1 : 1	130	24	None			
9		250 : 1 : 1	130	1	None			
10	**6**	500 : 1 : 2	80	24	5.1			
11		500 : 1 : 2	80	1	None			
12		250 : 1 : 1	130	24	17			
13		250 : 1 : 1	130	1	None			
14	**9**	250 : 1 : 1	130	24	65.4	15 160	16 480	1.43
15		250 : 1 : 1	130	1	None			
16	**11**	250 : 1 : 2	130	24	69.6	13 000	8820	1.37
17		250 : 1 : 2	130	1	None			
18	**12**	250 : 1 : 2	80	24	52	Oligomers		
19		250 : 1 : 2	130	24	64	6710	8120	1.92
20	**13**	250 : 1 : 2	80	24	41	Oligomers		
21		250 : 1 : 2	130	24	53	5590	6740	1.41

[a] Determined by ^{1}H NMR spectroscopy on crude reaction mixture. [b] From GPC. [c] Calculated from ($[\mathrm{Monomer}]_0/[\mathrm{OH}]_0$) × conv. (%) × Monomer molecular weight + Molecular weight of BnOH. [d] Reaction performed in air.

Table 4 ROP of rac-lactide using complexes **1**, **3**, **4**, **6**, **9** and **11–13**

Run	Catalyst	*r*-LA : Ti : BnOH	*T* (°C)	Time (h)	Conversion[a] (%)	M_n[b,c]	$M_{n\text{calc}}$[d]	M_w/M_n[b]
1	**1**	500 : 1 : 3	130	24	87	8190	21 000	1.29
2		500 : 1 : 3	130	1	33			
3	**3**	250 : 1 : 4	130	24	None	—	—	—
4	**4**	500 : 1 : 2	130	24	None			
5		500 : 1 : 2	130	1	None			
6		250 : 1 : 1	130	24	None			
7		250 : 1 : 1	130	1	None			
8	**6**	500 : 1 : 2	130	24	None			
9		500 : 1 : 2	130	1	None			
10		250 : 1 : 1	130	24	None			
11		250 : 1 : 1	130	1	None			
12	**9**	250 : 1 : 1	130	24	None			
13		250 : 1 : 1	130	1	None			
14	**11**	250 : 1 : 1	130	24	8.2			
15		250 : 1 : 1	130	1	None			
16	**12**	250 : 1 : 2	130	24	>99	4980	21 650	1.20
17	**13**	250 : 1 : 2	130	24	37	Liquid oligomers		

[a] Determined by ^{1}H NMR spectroscopy on crude reaction mixture. [b] From GPC. [c] Values corrected considering Mark–Houwink factor (0.58) from polystyrene standards in THF. [d] Calculated from ($[\text{Monomer}]_0/[\text{OH}]_0$) × conv. (%) × Monomer molecular weight + Molecular weight of BnOH.

Table 5 ε-CL/δ-VL co-polymerization using complexes **1**, **3**, **4**, **6**, **9** and **11–13**

Run	Catalyst	ε-CL:δ-VL : Ti : BnOH	Conversion[a] (%)	CL/VL[b]	M_n[c,d]	M_w/M_n[c]
1	**1**	250 : 250 : 1 : 3	67.6	40 : 60	7770	1.19
2	**3**	250 : 250 : 1 : 4	None	—	—	—
3	**4**	250 : 250 : 1 : 1	29.9	50 : 50	nd	nd
4	**6**	250 : 250 : 1 : 1	41.9	50 : 50	nd	nd
5	**9**	250 : 250 : 1 : 1	22.2	50 : 50	nd	nd
6	**11**	250 : 250 : 1 : 1	81.0	50 : 50	5185	1.47
7	**12**	250 : 250 : 1 : 2	>99	55 : 45	12 480	1.70
8	**13**	250 : 250 : 1 : 2	>99	60 : 40	13 960	1.84

Reaction conditions: Toluene, *T* = 130 °C, 24 h. [a] Determined by ^{1}H NMR spectroscopy on the crude reaction mixture based on ε-CL. [b] Determined by ^{13}C NMR. [c] From GPC. [d] Values corrected considering Mark–Houwink factor [($M_n \times \%_{CL} \times 0.56$) + ($M_n \times \%_{VL}$)] from polystyrene standards in THF.

polymer with low molecular weight and narrow polydispersity. The ^{1}H NMR spectroscopic analyses of the crude reaction mixture suggested a CL : VL ratio in the copolymer of 40 : 60. No conversion was achieved when employing complex **3** (run 2). Low conversions, spanning from 20 to 40% were observed by using the titanocalix[8]arene complexes **4**, **6**, and **9** (runs 3–5). In all cases, the CL : VL ratio was found to be *ca.* 1 : 1. However, the molecular weights of such co-polymers were too low to be detected by SEC, suggesting the occurrence of undesirable transesterification side-reactions resulting in the formation of light oligomers. Finally, good conversion was achieved by using **11** (81%, run 6). Similar to **1**, the catalyst was shown to incorporate ε-CL and δ-VL in 1 : 1 ratio. The average sequence length for CL was found to be 2.46 while the value for VL was 1.69, as observed by ^{13}C NMR spectroscopy (ESI, Fig. S17† and eqn (S1)–(S3)†).[26] The randomness degree for the co-polymer was 1.0, compatible with a purely random copolymer.[26a]

In the presence of the bi-phenolate complexes **12** and **13**, complete conversion was observed (runs 7 and 8), affording co-polymers with M_n spanning from 12 to 14 kDa with rather poor control (M_w/M_n *ca.*1.75). Also in this case, the co-polymer composition was analyzed by ^{13}C NMR spectroscopy. For the polymer isolated with **12**, the average sequence length was 2.10 and 2.05 for CL and VL, respectively (ESI, Fig. S18†), with a randomness degree of 0.97, compatible with a purely random co-polymer.[26a] A similar outcome was achieved with complex **13**; in fact, the average sequence lengths were 2.50 and 1.82 for CL and CL, respectively, with a randomness degree of 0.95 (ESI, Fig. S19†).

ε-CL/*r*-LA co-polymerization. None of the complexes proved to be active in the co-polymerization of ε-CL and *r*-LA at

130 °C. In most cases, both monomers were unreacted after 24 h. Nevertheless, 14% conversion of *r*-LA in PLA was achieved in the presence of **1**, as highlighted by ^{1}H NMR spectroscopy on the crude reaction mixture (see Fig. S20, ESI†).

Conclusion

The treatment of L^1H_6 with [$TiCl_4$] afforded complex **1**·4.5MeCN, in which two pseudo-octahedral titanium centres are bound to one calix[6]arene. A similar preparation conducted in THF resulted in the THF ring-opened product 2·4MeCN, containing an LH_4- (where LH_4 = *p-tert*-butylcalix[4]areneH_4) derived ligand resulted from impurities in L^1H_6. In the case of [TiF_4] (3 equiv.), reaction with L^1H_6 afforded the orange/red complex **3**·6.5MeCN, in which two Ti_2F_2 diamonds bridge the calixarenes, whilst two fluoride ions bridge the two diamonds. The reaction between L^2H_8, with [$TiCl_4$] led to $[(TiCl)_2(TiClNCMe)_2(\mu_3\text{-}O)_2(L^2)]$·1.5MeCN (**4**·1.5MeCN) and, from a similar preparation, to the co-crystallized complex $[Ti_4O_2Cl_4(MeCN)_2(L^2)][Ti_3Cl_6(MeCN)_5(OH_2)(L^2H_2)]$·$H_2O$·11MeCN (**5**·$H_2O$ 11MeCN). Extension of the L^2H_8 chemistry to [$TiBr_4$] afforded, depending on the stoichiometry, $[(TiBr)_2(TiBrNCMe)_2(\mu_3\text{-}O)_2(L^2)]$·6MeCN (**6**·6MeCN) or $[Ti(NCMe)_2Br]_2[Ti(O)Br_2(NCMe)][(L^2)]$·7.5MeCN (**7**·7.5MeCN), respectively. Interestingly, the use of [TiF_4] afforded complexes containing Ca^{2+} and Na^+, most likely deriving from drying agents, namely $[Ti_8CaF_{20}(OH_2)Na_2(MeCN)_4(L^2)_2]$·14MeCN (**8**·14MeCN), $[Na(MeCN)_2][Ti_8CaF_{20}NaO_{16}(L^2)_2]$·7MeCN (**9**·7MeCN) or $[Na]_6[Ti_8F_{20}Na(MeCN)_2(L^2)][Ti_8F_{20}Na(MeCN)_{0.5}(L^2)]$·15.5($C_2H_3N$) (**10**·15.5MeCN). By using [TiI_4], the ladder **11**·7.25CH_2Cl_2 was isolated. These complexes have been tested as catalysts in the ring opening polymerization (ROP) of ε-CL, δ-VL and *r*-LA, both in air and N_2. In the case of ε-CL, high temperatures (130 °C) over 24 h were required to achieve reasonable conversions for **1**, **9** and **11** (**3** and **6** were inactive). However, these metallocalix[*n*]arenes are out-performed by the diphenolates **12** and **13**, which doubtless reflects the accessiblity of the metal centres in the latter. In the case of δ-VL, the salts **9** and **10** as well as **12** and **13** perform best, whilst for *r*-LA, **1**, **12** and to a lesser extent **11**, **13** were active. For the copolymerization of ε-CL with δ-VL reasonable activity was exhibited by **1** and **11**, whilst conversions lower than 40% were observed with the other complexes; all afforded low molecular weight polymers. The copolymerization of ε-CL with *r*-LA was unsuccessful regardless of the catalyst employed. In general for these systems, more accessible metals centres (*e.g.* **1**, **12** and **13**) and the formation of salts (*e.g.* **9–11**) favours improved catalytic performance in the ROP of cyclic esters.

Experimental section

General

All manipulations were carried out under an atmosphere of dry nitrogen using conventional Schlenk and cannula techniques or in a conventional nitrogen-filled glove box. Hexane and toluene were refluxed over sodium. Acetonitrile was refluxed over calcium hydride. All solvents were distilled and degassed prior to use. IR spectra (nujol mulls, KBr windows) were recorded on a Nicolet Avatar 360 FT IR spectrometer; ^{1}H NMR spectra were recorded at room temperature on a Varian VXR 400 S spectrometer at 400 MHz or a Gemini 300 NMR spectrometer or a Bruker Advance DPX-300 spectrometer at 300 MHz. The ^{1}H NMR spectra were calibrated against the residual protio impurity of the deuterated solvent. Elemental analyses were performed by the elemental analysis service at the London Metropolitan University and in the Department of Chemistry, the University of Hull. All chemicals were purchased from either Sigma Aldrich or TCI UK.

Synthesis of $[Ti_2Cl_3(MeCN)_2(OH_2)(L^1H)]$ $[Ti_2Cl_3(MeCN)_3(L^1H)]$·4.5 MeCN (1·4.5 MeCN)

To L^2H_6 (2.00 g, 2.05 mmol) in toluene (30 mL) was added [$TiCl_4$] (0.71 mL, 6.50 mmol) and the system was refluxed for 12 h. On cooling, the volatiles were removed *in-vacuo*, and the residue was extracted into MeCN (30 mL). On standing at ambient temperature (*ca.* 10 °C) for 2 days, orange crystals of **1** formed. Yield 1.80 g, 64%. Sample dried under reduced pressure for 12 h (−4.5 MeCN). $C_{142}H_{175}Cl_6N_5O_{13}Ti_4$ requires C 66.51, H 6.88, N 2.73%. Found C 65.59, H 7.22, N 2.21%. IR: 3596w, 2727w, 2326w, 1635w, 1596w, 1364m, 1296m, 1259s, 1208s, 1112s, 1096s, 1022s, 928, 884s, 859m, 799s, 766m. ^{1}H NMR (C_6D_6): ^{1}H NMR ($CDCl_3$, 298 K) δ: 7.15–6.76 (m, 12H, aryl*H*), 6.36 (s, 1H, arylO*H*), 6.20 (s, 1H, Ti-O*H*), 4.74 (d, 2H, J = 12 Hz, *endo*-CH_2), 4.19 (d, 1H, J = 12 Hz, *endo*-CH_2), 4.33 (d, 1H, J = 12 Hz, *endo*-CH_2), 4.11 (d, 1H, J = 12 Hz, *endo*-CH_2), 3.57 (d, 4H, J = 12 Hz, *exo*-CH_2), 2.98 (d, 1H, J = 12 Hz, *exo*-CH_2), 2.01 (s, 12H, 4 uncoordinated MeCN), 1.29–1.01 (m, 54H, C(CH_3)$_3$), 0.50 (s, 6H, 2 coordinated MeCN).

Synthesis of $[Ti_4Cl_2(\mu_3\text{-}O)_2(NCMe)_2(L)_2(O(CH_2)_4Cl)_2]$·4MeCN (2·4MeCN)

Crystals of complex **2** suitable for X ray analysis were obtained in low yield (<5%) from the preparation of **1**. Due to the limited amount of sample (~5 mg), only ^{1}H NMR spectroscopy analysis could be performed. ^{1}H NMR (C_6D_6) δ: 7.20–7.05 (m, 16H aryl*H*), 5.43 (d, 4H, J = 13 Hz, *endo*-CH_2), 5.15 (d, 4H, J = 13 Hz, *endo*-CH_2), 4.97 (m, 4H, ClCH_2CH_2CH_2CH_2O–), 4.88 (m, 4H, ClCH_2CH_2CH_2CH_2O–), 4.10 (m, 4H *exo*-CH_2), 2.24 (m, 4H, ClCH_2CH_2CH_2CH_2O–), 1.98 (m, 4H, ClCH_2CH_2CH_2CH_2O–), 1.56–1.23 (m, 72H C(CH_3)).

Synthesis of $[(TiF)_2(\mu\text{-}F)L^1H]_2$·6.5MeCN (3·6.5MeCN)

To L^2H_6 (2.00 g, 2.05 mmol) in toluene (30 mL) was added [TiF_4] (0.76 g, 6.14 mmol) and the system was refluxed for 12 h. On cooling, the volatiles were removed *in-vacuo*, and the residue was extracted into MeCN (30 mL). On standing at ambient temperature at 0 °C for 2 days, orange/red crystals of **3** formed. Yield 1.75 g, 68%. $C_{132}H_{158}F_6O_{12}Ti_4$·3MeCN (sample dried *in vacuo* for 2 h, −3.5MeCN) requires C 70.07, H 7.12, N 1.78%. Found C 68.82, H 7.18, N 1.29%. IR: 3442bs, 2727w, 2671w, 1636m, 1600m, 1417m, 1392s, 1364s, 1297m, 1260s, 1201s, 1101s, 1020s, 932m, 886m, 860m, 799s, 767w, 680w,

588w, 559w, 545w, 463w, 438w. ^{1}H NMR ($CDCl_3$) δ: 7.24 (s, 8H, Ar*H*), 7.12 (s, 8H, Ar*H*), 6.99 (s, 8H, Ar*H*), 5.17 (d, J = 12 Hz, 15H, *endo*-CH_2), 4.00 (bs, 2H, –O*H*), 3.18 (d, J = 15 Hz, 12H, *exo*-CH_2), 2.00 (s, 18H, 6 coordinated MeCN), 1.26 (s, 54H, C(CH_3)), 1.16 (s, 54H, C(CH_3)). ^{19}F NMR ($CDCl_3$) δ: −2.13 (q, J = 49 Hz, 2F, Ti–F–Ti), −15.96 (t, J = 46 Hz, 4F, TiF_2).

Synthesis of $[(TiCl)_2(TiClNCMe)_2(\mu_3\text{-}O)_2(L^2)]\cdot 1.5MeCN$ (4·1.5MeCN)

As for **1**, but using L^2H_8 (2.00 g, 1.54 mmol) and [$TiCl_4$] (6.50 mL, 1.0 M in CH_2Cl_2, 6.50 mmol) affording **4** as small red prisms. Yield 2.13 g, 77%. Sample dried in value for 12 h (−1.5MeCN) $C_{92}H_{110}Cl_4N_2O_{10}Ti_4$ requires C 63.60, H 6.38, N 1.61%. Found C 62.87, H 6.71, N 1.43%. IR: 2319w, 2308w, 2289w, 2257w, 1648m, 1596s, 1393m, 1364m, 1291m, 1256s, 1196s, 1122m, 1105m, 1028m, 933s, 887s, 878s, 862s, 855s, 796m, 772w, 760w, 737w, 720m, 673w, 658w. ^{1}H NMR (C_6D_6) δ: 7.29 (s, 4H, aryl*H*), 7.08 (bs, 8H, aryl*H*), 7.04 (bs, 4H, aryl*H*), 5.62 (d, J = 12 Hz, 2H, *endo*-CH_2), 5.11 (d, J = 12 Hz, 4H, *endo*-CH_2), 4.21 (d, J = 12 Hz, 2H, *endo*-CH_2), 3.87 (d, J = 12 Hz, 2H, *exo*-CH_2), 3.40 (d, J = 12 Hz, 4H, *exo*-CH_2), 2.68 (d, J = 12 Hz, 2H, *exo*-CH_2), 1.12 (s, 36H, C(CH_3)$_3$), 1.04 (s, 36H, C(CH_3)$_3$), 0.50 (s, 27H, 9MeCN).

Synthesis of $[Ti_4O_2Cl_4(MeCN)_2(L^2)][Ti_3Cl_6(MeCN)_5(OH_2)(L^2H_2)][OH_2]\cdot 11MeCN$ (5·11MeCN)

As for **4**, but using L^2H_8 (1.00 g, 0.77 mmol) and [$TiCl_4$] (3.08 mL, 1.0 M in CH_2Cl_2, 3.08 mmol) affording **5** as small red prisms. Yield 1.03 g, 66%. Sample dried for 24 h *in vacuo* (−14MeCN) $Ti_7Cl_{10}N_7O_{19}C_{190}H_{233}\cdot OH_2$ requires C 63.07, H 6.50, N 1.60%. Found: C 62.87, H 6.71, N 1.43%. IR: 2313w, 2286w, 2249w, 1598w, 1577w, 1459m, 1416m, 1392s, 1364s, 1292s, 1259s, 1208s, 1158w, 1119m, 1102m, 1048w, 1024m, 964w, 948w, 929m, 886m, 874m, 860m, 832w, 816w, 794 m, 756w, 722 m, 699w. ^{1}H NMR (C_6D_6) δ: 7.29 (s, 4H, aryl*H*), 7.07 (bs, 8H, aryl*H*), 7.03 (s, 4H, aryl*H*), 5.62 (d, J = 13 Hz, 2H, *endo*-CH_2), 5.08 (d, J = 13 Hz, 4H, *endo*-CH_2), 4.17 (d, J = 13 Hz, 2H, *endo*-CH_2), 3.87 (d, J = 13 Hz, 2H, *exo*-CH_2), 3.38 (d, J = 13 Hz, 4H, *exo*-CH_2), 2.66 (d, J = 13 Hz, 2H, *exo*-CH_2), 1.22 (s, 36H, C(CH_3)$_3$), 1.03 (s, 36H, C(CH_3)$_3$), 0.50 (s, 3H, MeCN coordinated).

Synthesis of $[(TiBr)_2(TiBrNCMe)_2(\mu_3\text{-}O)_2(L^2)]\cdot 6MeCN$ (6·6MeCN)

As for **1**, but using L^2H_8 (2.00 g, 1.54 mmol) and [$TiBr_4$] (2.26 g, 6.16 mmol), affording **6** as orange/brown prisms. Yield 2.31 g, 69%. $C_{92}H_{110}Br_4N_2O_{10}Ti_4\cdot 6MeCN$ requires C 57.79, H 5.97, N 5.19%. Found: C 58.77, H 6.39, N 4.88%. IR: 2361w, 2336w, 2313w, 2251w, 1633w, 1596w, 1415w, 1365s, 1291m, 1260s, 1198s, 1103s, 1026m, 932 m, 880s, 858s, 797s, 768w, 722 m, 684w. ^{1}H NMR (C_6D_6; sample required heating for 3 h prior to running in order to increase solubility) δ: 7.07–7.02 (m, 16H, Ar*H*), 5.70 (d, J = 13 Hz, 2H, *endo*-CH_2), 5.18 (d, J = 13 Hz, 4H, *endo*-CH_2), 4.22 (d, J = 13 Hz, 2H, *endo*-CH_2), 3.86 (d, J = 13 Hz, 2H, *exo*-CH_2), 3.42 (d, J = 13 Hz, 4H, *exo*-CH_2), 2.64 (d, J = 13 Hz, 2H, *exo*-CH_2), 2.05 (s, 1.5H, 0.5 uncoordinated MeCN), 1.21 (s, 36H, C(CH_3)$_3$), 1.10 (s, 36H, C(CH_3)$_3$), 0.54 (s, 18H, coordinated MeCN).

Synthesis of $[Ti(NCMe)_2Br]_2[Ti(OH_2)Br_2(NCMe)](L^2)]\cdot 7.5MeCN$ (7·7.5MeCN)

As for **1**, but using L^2H_8 (1.00 g, 0.77 mmol) and [$TiBr_4$] (0.85 g, 2.31 mmol), affording **7** as orange/brown prisms. Yield 1.53 g, 81%. Sample dried under reduced pressure for 16 h (−6.5 MeCN). $C_{98}H_{123}Br_6N_5O_9Ti_3\cdot MeCN$ requires C 55.11, 5.83, N 3.86%. Found: C 56.89, H 5.74, N 3.78%. IR: 3380m, 2726w, 2671w, 2363w, 2342w, 2314w, 2286w, 2250w, 1744w, 1648w, 1597w, 1572w, 1377s, 1301w, 1288w, 1259m, 1201m, 1102m, 1028m, 934 m, 882 m, 872 m, 859 m, 799 m, 775w, 721w, 702w, 680w, 622w, 606w. ^{1}H NMR (C_6D_6) δ: 7.17–6.96 (m, 16H, Ar*H*), 5.75 (d, J = 12 Hz, 2H, *endo*-CH_2), 5.23–5.39 (m, 2H, *endo*-CH_2), 5.28 (d, J = 12 Hz, 2H, *endo*-CH_2), 4.62 (d, J = 12 Hz, 2H, *endo*-CH_2), 4.18 (m, 2H, *exo*-CH_2), 4.01 (d, J = 12 Hz, 2H, *exo*-CH_2), 3.64–3.50 (m, 2H *exo*-CH_2), 3.39–3.34 (m, 2H, *exo*-CH_2), 1.25 (s, 36H, C(CH_3)$_3$), 1.03 (s, 36H, C(CH_3)$_3$), 0.83 (s, 9H, co-ordinated MeCN). O*H* signals not found.

Synthesis of $[Ti_8CaF_{20}(OH_2)(Na_2(MeCN)_4)(L^2)_2]\cdot 14MeCN$ (8·14MeCN)

L^2H_8 (2.00 g, 1.54 mmol) and [TiF_4] (0.76 g, 6.16 mmol) were combined in toluene (30 mL) and the system was refluxed for 12 h. On cooling, volatiles were removed *in-vacuo*, and the residue was extracted into MeCN (30 mL). Prolonged standing at 0 °C afforded **8** as red, blade-like crystals. Yield: 1.87 g, 58%. The sample was dried under reduced pressure for 16 h. $C_{184.67}H_{234.02}CaF_{20}N_4Na_2O_{17}Ti_8\cdot$(−14MeCN) requires C 61.13, H 6.49, N 1.54%. Found: C 60.73, H 6.34, N 1.89%. IR: 1648w, 1303w, 1261s, 1199w, 1095s, 1020s, 929w, 873w, 859w, 800s, 753w, 722w, 660w. ^{1}H NMR (C_6D_6) δ: 7.35–7.12 (m, 16H, Ar*H*), 7.10–6.98 (m, 16H, Ar*H*), 5.75 (m, 4H, *endo*-CH_2), 5.50 (m, 8H, *endo*-CH_2), 5.08–4.95 (m, 4H *endo*-CH_2), 4.02–3.82 (m, 4H, *exo*-CH_2), 3.43 (m, 4H, *exo*-CH_2), 3.26 (m, 4H, *exo*-CH_2), 3.08 (m, 4H, *exo*-CH_2), 1.40–1.21 (m, 72H, C(CH_3)$_3$), 1.20–1.07 (m, 72H, C(CH_3)$_3$), 0.50 (s, 12H, 4 coordinated MeCN). ^{19}F NMR (C_6D_6) δ: −4.25 (bs, 2F), −7.58 (bs), −8.89 (bs), −9.73 (bs) −11.1 (bs), −13.2 (bs), −17.2 (bs), −20.2 (bs), −22.1 (bs), −27.9 (bs).

Synthesis of $[Na(MeCN)_2][Ti_8CaF_{20}NaO_{16}(L^2)_2]\cdot 7(MeCN)$ (9·7MeCN)

As for **8**, affording **9** as red blade-like crystals. Yield: 46%. $C_{176}H_{208}CaF_{20}Na_2O_{16}Ti_8\cdot 9(C_2H_3N)$ requires C 61.41, H 6.21, N 2.64%. Found C 60.65, H 6.69, N 2.48%. IR: 1651w, 1300w, 1257s, 1200w, 1089s, 1015s, 925w, 871w, 857w, 798s, 756w, 727w, 663w. ^{1}H NMR (C_6D_6) δ: 7.34–7.09 (m, 16H, Ar*H*), 7.03–6.86 (m, 16H, Ar*H*), 6.26–6.09 (m, 4H, *endo*-CH_2), 5.94–5.80 (m, 8H, *endo*-CH_2), 5.21–4.93 (m, 4H *endo*-CH_2), 4.50–4.44 (m, 4H, *exo*-CH_2), 4.40–4.35 (m, 4H, *exo*-CH_2), 4.19–4.15(m, 4H, *exo*-CH_2), 3.99–3.84 (m, 4H, *exo*-CH_2), 2.11 (s, 21H, 7coordinated MeCN) 1.47–1.37 (m, 72H, C(CH_3)$_3$), 1.32–1.28 (m, 72H, C(CH_3)$_3$), 0.58 (s, 6H, 2 coordinated MeCN). ^{19}F NMR (C_6D_6) δ: −3.50 (bs, 2F), −6.72 (bs, 2F), −6.90

Table 6 Crystallographic Data

Compound	**1**·4.5(C_2H_3N)	**2**·4(C_2H_3N)	**3**·6.5(C_2H_3N)	**4**·1.5(C_2H_3N)
Formula	$[C_{72}H_{87}Cl_3N_3O_6Ti_2]$ $[C_{70}H_{88}Cl_3N_2O_7Ti_2]$·4.5($C_2H_3N$)	$C_{100}H_{126}Cl_4N_2O_{12}Ti_4$·4($C_2H_3N$)	$C_{132}H_{158}F_6O_{12}Ti_4$·6.5($C_2H_3N$)	$C_{92}H_{110}Cl_4N_2O_{10}Ti_4$·1.5($C_2H_3N$)
Formula weight	2748.90	2045.64	2509.02	1798.79
Crystal system	Triclinic	Triclinic	Monoclinic	Orthorhombic
Space group	$P\bar{1}$	$P\bar{1}$	$C2/c$	$P2_12_12_1$
a (Å)	12.7071(4)	11.1401(2)	24.7656(7)	18.7623(3)
b (Å)	24.5925(4)	15.00590(15)	22.6045(5)	19.3331(3)
c (Å)	25.2999(7)	16.5752(3)	24.6564(6)	26.9512(3)
α (°)	104.399(2)	104.2611(12)	90	90
β (°)	96.177(2)	93.0977(15)	90.923(2)	90
γ (°)	91.761(2)	98.7122(13)	90	90
V (Å^3)	7599.8(3)	2642.36(7)	13 801.2(6)	9776.1(2)
Z	2	1	4	4
Temperature (K)	100(2)	100(2)	100(2)	100(2)
Wavelength, λ (Å)	1.54178	1.54178	0.71073	1.54178
Calculated density (g cm^{-3})	1.201	1.286	1.208	1.222
Absorption coefficient, μ (mm^{-1})	3.17	3.90	0.29	4.13
Transmission factors (min./max.)	0.694, 1.000	0.917, 1.000	0.568, 1.000	0.724, 1.000
Crystal size (mm^3)	0.26 × 0.05 × 0.01	0.07 × 0.06 × 0.05	0.19 × 0.10 × 0.06	0.10 × 0.05 × 0.02
θ(max) (°)	68.2	68.3	27.5	68.2
Reflections measured	102 365	99 465	69 296	94 785
Unique reflections	27 528	19 474	15 792	17 801
R_{int}	0.103	0.024	0.082	0.049
Reflections with $F^2 > 2\sigma(F^2)$	14 620	17 743	9515	15 039
Number of parameters	1964	645	824	1175
R_1 [$F^2 > 2\sigma(F^2)$]	0.126	0.067	0.083	0.063
wR_2 (all data)	0.380	0.190	0.245	0.180
GOOF, S	1.03	1.05	1.07	1.02
Largest difference peak and hole (e Å^{-3})	1.41 and −0.84	2.55 and −1.20	0.91 and −0.70	0.94 and −0.48

Compound	**5**·(H_2O)·11(C_2H_3N)	**6**·6(C_2H_3N)	**7**·7.5(C_2H_3N)	**8**·14(C_2H_3N)
Formula	$[C_{92}H_{110}Cl_4N_2O_{10}Ti_4][C_{98}H_{123}Cl_6N_5O_9Ti_3]$·$OH_2$·11($C_2H_3N$)	$C_{92}H_{110}Br_4N_2O_{10}Ti_4$·6($C_2H_3N$)	$C_{98}H_{123}Br_6N_5O_9Ti_3$·7.5($C_2H_3N$)	$C_{184.67}H_{234.02}CaF_{20}N_4Na_2O_{17}Ti_8$·14($C_2H_3N$)
Formula weight	4078.23	2161.38	2446.07	4195.75
Crystal system	Triclinic	Monoclinic	Monoclinic	Monoclinic
Space group	$P\bar{1}$	$P2_1/c$	$P2_1/n$	$P2_1/m$
a (Å)	18.0637(2)	21.02305(10)	21.5584(2)	20.9093(17)
b (Å)	20.6914(3)	17.27686(8)	26.9199(3)	23.0191(7)
c (Å)	31.5620(2)	29.70228(14)	21.6443(2)	23.6904(10)
α (°)	103.4502(9)	90	90	90
β (°)	97.2290(8)	102.5511(5)	95.7763(7)	99.755(5)
γ (°)	99.0055(11)	90	90	90
V (Å^3)	11 168.9(2)	10 530.42(9)	12 497.5(2)	11 237.6(11)
Z	2	4	4	2
Temperature (K)	100(2)	100(2)	100(2)	100(2)
Wavelength, λ (Å)	1.54178	1.54178	1.54178	0.71073
Calculated density (g cm^{-3})	1.213	1.363	1.300	1.240
Absorption coefficient, μ (mm^{-1})	3.62	4.74	4.28	0.37

Table 6 *(Contd.)*

Compound	**5**·(H_2O)·11(C_2H_3N)	**6**·6(C_2H_3N)	**7**·7.5(C_2H_3N)	**8**·14(C_2H_3N)
Transmission factors (min./max.)	0.757, 1.000	0.595, 1.000	0.539, 1.000	0.373, 1.000
Crystal size (mm^3)	0.10 × 0.10 × 0.03	0.24 × 0.14 × 0.08	0.19 × 0.09 × 0.01	0.17 × 0.04 × 0.02
θ(max) (°)	68.3	68.3	68.2	27.5
Reflections measured	204 131	100 958	126 455	108 461
Unique reflections	40 624	19 224	22 797	26 376
R_{int}	0.075	0.027	0.054	0.151
Reflections with $F^2 > 2\sigma(F^2)$	26 722	18 352	17 330	8680
Number of parameters	2353	1278	1293	1389
R_1 [$F^2 > 2\sigma(F^2)$]	0.078	0.036	0.091	0.115
wR_2 (all data)	0.242	0.095	0.293	0.399
GOOF, S	1.06	1.04	1.04	0.96
Largest difference peak and hole (e $Å^{-3}$)	1.96 and −0.74	0.89 and −0.66	2.76 and −1.42	1.15 and −0.68

Compound	**9**·9(C_2H_3N)	**10**·15.5(C_2H_3N)	**11**·7.25CH_2Cl_2	**12**·hexane
Formula	$C_{176}H_{208}CaF_{20}Na_2O_{16}Ti_8$·9($C_2H_3N$)	$[Na]_6[C_{180}H_{214}F_{20}N_2NaO_{16}Ti_8][C_{177}H_{209.5}F_{20}N_{0.5}NaO_{16}Ti_8]$·15.5($C_2H_3N$)	$C_{92}H_{110}I_4N_2O_{10}Ti_4$·7.25($CH_2Cl_2$)	$C_{30}H_{44}Br_2O_2Ti$·C_6H_{14}
Formula weight	3798.16	7608.11	2718.73	730.54
Crystal system	Monoclinic	Triclinic	Monoclinic	Orthorhombic
Space group	$P2_1/c$	$P\bar{1}$	$P2_1/c$	$Cmc2_1$
a (Å)	23.4034(4)	20.3323(2)	29.2721(4)	16.4524(3)
b (Å)	22.4883(3)	28.7880(3)	9.52188(14)	12.3781(2)
c (Å)	37.6555(7)	36.5201(3)	43.6988(6)	18.0939(3)
α (°)	90	96.9496(8)	90	90
β (°)	100.267(2)	99.4528(9)	103.0731(13)	90
γ (°)	90	97.6499(9)	90	90
V ($Å^3$)	19 500.9(6)	20 673.9(4)	11 864.3(3)	3684.81(11)
Z	4	2	4	4
Temperature (K)	100(2)	100(2)	100(2)	100(2)
Wavelength, λ (Å)	1.54178	1.54178	1.54178	0.71073
Calculated density (g cm^{-3})	1.294	1.222	1.522	1.317
Absorption coefficient, μ (mm^{-1})	3.59	3.21	13.80	2.43
Transmission factors (min./max.)	0.662, 1.000	0.649, 1.000	0.241, 0.708	0.533, 1.000
Crystal size (mm^3)	0.20 × 0.04 × 0.02	0.32 × 0.15 × 0.02	0.17 × 0.04 × 0.03	0.22 × 0.06 × 0.04
θ(max) (°)	68.2	68.3	68.3	28.7
Reflections measured	176 468	340 686	103 662	31 640
Unique reflections	35 581	75 256	21 509	4905
R_{int}	0.100	0.096	0.152	0.037
Reflections with $F^2 > 2\sigma$ (F^2)	16 907	47 212	16 795	4716
Number of parameters	2275	4870	1290	253
R_1 [$F^2 > 2\sigma$ (F^2)]	0.084	0.099	0.099	0.027
wR_2 (all data)	0.266	0.320	0.275	0.069
GOOF, S	1.02	1.03	1.04	1.05
Largest difference peak and hole (e $Å^{-3}$)	0.92 and −0.71	1.32 and −0.55	1.56 and −1.89	0.54 and −0.72

(bs, 2F), −8.04 (bs, 2F), −11.40 (bs, 2F), −13.74 (bs, 2F), −17.40 (bs, 2F), −19.61 (bs, 2F), −21.94 (bs, 2F), −27.32(bs, 2F).

Synthesis of $[Na]_6[C_{180}H_{214}F_{20}NaN_2O_{16}Ti_8][C_{177}H_{209.5}F_{20}NaN_{0.5}O_{16}Ti_8]\cdot 15.5(C_2H_3N)$ (10·15.5MeCN)

As for **8**, except that both the toluene and acetonitrile were dried over activated molecular sieves, to afforded **10** in 61% yield. Sample dried under reduced pressure for 3 h (−7.5MeCN). $C_{357}H_{423.5}F_{40}N_{2.5}Na_8O_{32}Ti_{16}\cdot 8(C_2H_3N)$ requires C 61.37, H 6.18, N 2.01%. Found: C 61.96, H 6.42, N 2.11%. IR: 2727w, 1598w, 1301m, 1260s, 1197m, 1020s, 929 m, 855 m, 798s, 752 m, 102w, 672w, 619 m, 590 m, 561 m, 541 m, 500 m. ^{1}H NMR ($CDCl_3$) δ: 7.64–7.57 (m, 16H, Ar*H*), 7.30–7.26 (m, 16H, Ar*H*), 4.67–4.62 (m, 4H, *endo*-CH_2), 4.52–4.45 (m, 4H, *endo*-CH_2), 3.99–3.96 (m, 8H *endo*-CH_2), 3.44–3.99 (m, 8H, *exo*-CH_2), 3.24–3.21 (m, 4H, *exo*-CH_2), 2.94–2.90 (m, 4H, *exo*-CH_2), 1.30–1.19 (m, 72H, C(CH_3)$_3$), 1.09–0.98 (m, 72H, C(CH_3)$_3$). ^{19}F NMR ($CDCl_3$ δ: −3.78 (m, 2F), −6.78 (m, 1F), −8.61 (m, 2F), −10.0 (m, 2F), −11.7 (m, 4F), −13.5 (m, 2F), −15.2 (m, 1F), −19.9 (m, 2F), −23.2 (m, 2F), −32.3 (m, 2F).

Synthesis of $[(TiI)_2(TiINCMe)_2(\mu_3\text{-}O)_2(L^2)]\cdot 7.25CH_2Cl_2$ (11·7.25CH_2Cl_2)

As for **1**, but using L^2H_8 (2.00 g, 1.54 mmol) and [TiI_4] (3.59 g, 6.46 mmol). Extraction into CH_2Cl_2 (30 mL) afforded upon prolonged standing at 0 °C red blocks of (**11**·7.25CH_2Cl_2). Yield: 2.22 g, 53%. $C_{92}H_{110}I_4N_2O_{10}Ti_4\cdot 7.25(CH_2Cl_2)$ C 44.08, H 4.63, N 1.07%. Found: C 42.80, H 4.87, N 0.55%. IR: 2720w, 1650w, 1300, 1265m, 1190w, 1090m, 1015m. 920w, 870w, 859w, 790 m, 715w. ^{1}H NMR (C_6D_6) δ: 7.31 (s, 4H, aryl*H*), 7.10 (bs, 8H, aryl*H*), 7.07 (bs, 4H, aryl*H*), 5.70 (d, J = 12 Hz, 2H, *endo*-CH_2), 5.08 (d, J = 12 Hz, 4H, *endo*-CH_2), 4.15 (d, J = 12 Hz, 2H, *endo*-CH_2), 3.84 (d, J = 12 Hz, 2H, *exo*-CH_2), 3.48 (d, J = 12 Hz, 4H, *exo*-CH_2), 2.63 (d, J = 12 Hz, 2H, *exo*-CH_2), 1.08 (s, 36H, C(CH_3)$_3$), 1.00 (s, 36H, C(CH_3)$_3$).

Synthesis of [Ti(Br)$_2$(6,6′-(ethane-1,1-diyl)bis(2,4-di-*tert*-butylphenolate)]·hexane (12 hexane)

To a solution of 6,6′-(ethane-1,1-diyl)bis(2,4-di-*tert*-butylphenol) (1.00 g, 2.28 mmol) in hexane (30 mL), [$TiBr_4$] (0.84 g, 2.28 mmol) was added and the mixture was stirred at 60 °C for 16 h. Upon cooling to room temperature, **12** was obtained as a red solid, which was recovered by filtration, washed with hexane (2 × 10 mL) and dried in vacuum at room temperature for 16 h (hexane). Yield 1.30 g, 88%. $C_{30}H_{44}Br_2O_2Ti$ requires C 55.92, H 6.88%. Found C 55.69, H 7.05% ^{1}H NMR ($CDCl_3$) δ: 7.45 (d, J = 2.5 Hz, 2H, Ar*H*), 7.20 (d, J = 2.5 Hz, 2H, Ar*H*), 4.15 (q, J = 6.6 Hz, 1H, C*H*(CH$_3$)), 1.74 (d, J = 6.9 Hz, 3H, CH_3), 1.51 (s, 18H, C(CH_3)$_3$), 1.32 (s, 18H, C(CH_3)$_3$). IR: 1223m, 1198m, 1100 w, 925 m, 630 w, 480 m, 440 w, 415 m, 360 w. Single crystals suitable for X-ray diffraction were obtained from the mother liquor upon standing at room temperature for 2 days.

Synthesis [Ti(I)$_2$(6,6′-(ethane-1,1-diyl)bis(2,4-di-*tert*-butylphenolate)]·(13)

As for **11**, but using 6,6′-(ethane-1,1-diyl)bis(2,4-di-*tert*-butylphenol) (0.50 g, 1.14 mmol) with [TiI_4] (0.63 g, 1.14 mmol) in hexane (15 mL) affording **13** as a red solid. Yield 0.70 g, 83%. $C_{30}H_{44}I_2O_2Ti$ requires C 48.80, H 6.01. Found C 49.43, H 6.66%. ^{1}H NMR ($CDCl_3$) δ: 7.45 (d, J = 2.3 Hz, 2H, Ar*H*), 7.21 (d, J = 2.4 Hz, 2H, Ar*H*), 3.92 (q, J = 6.6 Hz, 1H, C*H*(CH$_3$)), 1.68 (d, J = 6.9 Hz, 3H, CH_3), 1.58 (s, 18H, C(CH_3)$_3$), 1.32 (s, 18H, C(CH_3)$_3$). IR: 1225m, 1195m, 1090 w, 922 m, 625 w, 477 m, 443 w, 410 m, 363 w.

Ring open polymerization (ROP) procedures

Typical polymerization procedures are as follows. Under nitrogen atmosphere, a Schlenk tube was charged with a toluene solution of the catalyst (10 mM) and the required amount of a toluene solution of benzyl alcohol (18 mM). The mixture was stirred for 2 min at room temperature, then the monomer (4.5 mmol) along with 1.5 mL toluene was added. The mixture was then placed into an oil bath pre-heated to the required temperature, and the solution was stirred for the prescribed time. The reaction was then quenched by addition of an excess of glacial acetic acid (0.2 mL) into the solution, and the resultant solution was then poured into methanol (200 mL). The resultant polymer was then collected on filter paper and dried *in vacuo*.

Crystal structure determinations

Crystallographic data for all structures is summarized in Table 6 and the ESI,† and full details are provided in the deposited cifs. Diffraction data for all structures was collected using Cu-Kα radiation except **8**·14MeCN and **12**·C_6H_{14} for which Mo-Kα radiation was used. A rotating anode X-ray source and Hypix 6000 detector Rigaku AFC11 diffractometer were employed in all cases.[27] Data were corrected for Lp effects and for absorption.[28] The structures were solved by a dual-space, charge flipping algorithm and refined by full matrix least-squares on F^2 values.[29,30] In common with most large ^{t}BuCalix[n]arene metal structures, disorder was observed in several ^{t}Bu groups and the solvent of crystallisation. In each case the disorder was modelled with restraints in geometrical and anisotropic displacement parameters. When point atom modelling was no longer possible due to severe disorder problems, the Platon Squeeze procedure was used to model the affected regions as diffuse areas of electron density.[21a,b] Details of the specific disorder modelling employed for each structure is given in the ESI.† CCDC 1973130–1973136, 1973364–1973366, and 2009076–2009077 contain the supplementary crystallographic data for this paper.†

Conflicts of interest

There are no conflicts to declare.

Acknowledgements

CR thanks the EPSRC for funding (EP/R023816/1), and the EPSRC National Crystallography Service at Southampton (UK) and the EPSRC Mass Spectrometry Service, Swansea (UK) for data.

Notes and references

1 See for example; (*a*) M. Delferro and T. J. Marks, *Chem. Rev.*, 2011, **111**, 2450; (*b*) C. Redshaw, *Catalysts*, 2017, **7**, 165.

2 (*a*) D. M. Homden and C. Redshaw, *Chem. Rev.*, 2008, **108**, 5086; (*b*) D. J. Hernández and I. Castillo, *Current Trends in X-ray Crystallography*, ed. A. Chandrasekaran, InTech, 2011. ISBN: 978-953-307-754-3; (*c*) Y. Li, K.-Q. Zhao, C. Redshaw, B. A. Martínez Ortega, A. Y. Nuñez and T. A. Hanna, Coordination Chemistry and Applications of Phenolic Calixarene–metal Complexes, Patai's Chemistry of Functional Groups, Wiley, 2014.

3 (*a*) S. Steyer, C. Jeunesse, D. Armspach, D. Matt and J. Harrowfield, in *Calixarenes*, ed. Z. Asfari, V. BÖhmer, J. Harrowfield and J. Vicens, Kluwer Academic Publishers, Dordrecht, 2001, ch. 28; (*b*) C. Floriani and R. Floriani-Moro, *Adv. Organomet. Chem.*, 2001, **47**, 167; (*c*) W. Sliwa, *Croat. Chem. Acta*, 2002, **75**, 131; (*d*) P. D. Harvey, *Coord. Chem. Rev.*, 2002, **233**, 289; (*e*) A. J. Petrella and C. L. Raston, *J. Organomet. Chem.*, 2004, **689**, 4125; (*f*) N. Kotzan and A. Vigalok, *Supramol. Chem.*, 2008, **20**, 129; (*g*) S. Siddiqui and P. J. Cragg, *Mini-Rev. Org. Chem.*, 2009, **4**, 283.

4 (*a*) C. D. Gutsche, *Calixarenes*, The Royal Society of Chemistry, Cambridge, England, 1989; (*b*) A. Arduini and A. Casnati, in *Macrocycle Synthesis*, ed. D. Parker, Oxford University Press, 1996, ch. 7.

5 C. Redshaw, *Coord. Chem. Rev.*, 2003, **244**, 45.

6 For early examples see. (*a*) M. M. Olmstead, G. Sigel, H. Hope, X. Xu and P. P. Power, *J. Am. Chem. Soc.*, 1985, **107**, 8087; (*b*) A. Zanotti-Gerosa, E. Solari, L. Giannini, C. Floriani, N. Re, A. Chiesi-Villa and C. Rizzoli, *Inorg. Chim. Acta*, 1998, **270**, 298; (*c*) W. Clegg, M. R. J. Elsegood, V. C. Gibson and C. Redshaw, *Dalton Trans.*, 1998, 3037; (*d*) U. Radius, *Inorg. Chem.*, 2001, **40**, 6637; (*e*) F. A. Cotton, E. V. Dikarev, C. A. Murillo and M. A. Petrukhina, *Inorg. Chim. Acta*, 2002, **332**, 41.

7 (*a*) C. Redshaw and M. R. J. Elsegood, *Inorg. Chem.*, 2000, **39**, 5164–5168; (*b*) C. Redshaw and M. R. J. Elsegood, *Polyhedron*, 2000, **19**, 2657; (*c*) V. C. Gibson, C. Redshaw and M. R. J. Elsegood, *J. Chem. Soc., Dalton Trans.*, 2001, 767; (*d*) C. Redshaw and M. R. J. Elsegood, *Eur. J. Inorg. Chem.*, 2003, 2071; (*e*) C. Redshaw, D. H. Homden, D. L. Hughes, J. A. Wright and M. R. J. Elsegood, *Dalton Trans.*, 2009, 1231; (*f*) C. Redshaw, M. Walton, K. Michiue, Y. Chao, A. Walton, P. Elo, V. Sumerin, C. Jiang and M. R. J. Elsegood, *Dalton Trans.*, 2015, **44**, 12292.

8 V. C. Gibson, C. Redshaw and M. R. J. Elsegood, *Chem. Commun.*, 2002, 1200.

9 C. Redshaw, M. J. Walton, D. S. Lee, C. Jiang, M. R. J. Elsegood and K. Michiue, *Chem. – Eur. J.*, 2015, **21**, 5199.

10 Y. Li, K.-Q. Zhao, C. Feng, M. R. J. Elsegood, T. J. Prior, X. Sun and C. Redshaw, *Dalton Trans.*, 2014, **43**, 13612.

11 J. D. Ryan, K. J. Gagnon, S. J. Teat and R. D. McIntosh, *Chem. Commun.*, 2016, **52**, 9071.

12 M. Frediani, D. Sémeril, D. Matt, L. Rosi, P. Frediani, F. Rizzolo and A. M. Papini, *Int. J. Polym. Sci.*, 2010, 490724, 6 pages.

13 M. Frediani, D. Sémeril, A. Marrioti, L. Rosi, P. Frediani, L. Rosi, D. Matt and L. Toupet, *Macromol. Rapid Commun.*, 2008, **209**, 1554.

14 Z. Sun, Y. Zhao, O. Santoro, M. R. J. Elsegood, E. V. Bedwell, K. Zahra, A. Walton and C. Redshaw, *Catal.: Sci. Technol.*, 2020, **10**, 1619.

15 O. Santoro and C. Redshaw, *Catalysts*, 2020, **10**, 210.

16 C. Redshaw, M. Rowan, D. M. Homden, M. R. J. Elsegood, T. Yamato and C. Pèrez-Casas, *Chem. – Eur. J.*, 2007, **13**, 10129.

17 (*a*) Y. Yu, Y. Zhang and R. Ling, *Synth. Commun.*, 1993, **23**, 1973; (*b*) A. Solovyev, E. Lacôte and D. P. Curran, *Dalton Trans.*, 2013, **42**, 695; (*c*) S. L. Borkowsky, R. F. Jordan and G. D. Hinch, *Organometallics*, 1991, **10**, 1268; (*d*) T. L. Breen and D. W. Stephan, *Inorg. Chem.*, 1992, **31**, 4019; (*e*) J. P. Campbell and W. L. Gladfelter, *Inorg. Chem.*, 1997, **36**, 4094; (*f*) A. Mommertz, R. Leo, W. Massa, K. Harms and K. Dehnicke, *Z. Anorg. Allg. Chem.*, 1998, **624**, 1647; (*g*) B. Birkmann, T. Voss, S. J. Geier, M. Ullrich, G. Kehr, G. Erker and D. W. Stephan, *Organometallics*, 2010, **29**, 5310.

18 L. A. Wright, E. G. Hope, G. A. Solan, W. B. Cross and K. Singh, *Organometallics*, 2016, **35**, 1183.

19 (*a*) G. D. Andreetti, G. Calestani, F. Ugozzoli, A. Arduini, E. Ghidini, A. Pochini and R. Ungaro, *J. Inclusion Phenom.*, 1987, **5**, 123; (*b*) W. Clegg, M. R. J. Clegg, S. J. Teat, C. Redshaw and V. C. Gibson, *J. Chem. Soc., Dalton Trans.*, 1998, 3037.

20 D. M. Miller-Shakesby, S. Nigam, D. L. Hughes, E. Lopez-Estelles, M. R. J. Elsegood, C. J. Cawthorne, S. J. Archibald and C. Redshaw, *Dalton Trans.*, 2018, **47**, 8992.

21 (*a*) P. v. d. Sluis and A. L. Spek, *Acta Crystallogr., Sect. A: Found. Crystallogr.*, 1990, **46**, 194; (*b*) A. L. Spek, *Acta Crystallogr., Sect. C: Struct. Chem.*, 2015, **71**, 9.

22 (*a*) H. W. Roesky, M. Sotoodeh and M. Noltemeyer, *Angew. Chem., Int. Ed. Engl.*, 1992, **31**, 864; (*b*) A. Pevec, A. Demsar, V. Gramlich, S. Petricek and H. W. Roesky, *J. Chem. Soc., Dalton Trans.*, 1997, **151**, 2215; (*c*) F. Q. Liu, D. Stalke and H. W. Roesky, *Angew. Chem., Int. Ed. Engl.*, 1995, **34**, 1872.

23 A. Arbaoui, C. Redshaw and D. L. Hughes, *Chem. Commun.*, 2008, 4717.

24 D. Takeuchi, T. Nakamura and T. Aida, *Macromolecules*, 2000, **33**, 725.
25 (*a*) C. Ludwig and M. R. Viant, *Phytochem. Anal.*, 2010, **21**, 22; (*b*) M. J. Walton, S. J. Lancaster and C. Redshaw, *ChemCatChem*, 2014, **6**, 1892.
26 (*a*) Q. Hu, S.-Y. Jie, P. Braunstein and B.-G. Lia, *Chin. J. Polym. Sci.*, 2020, **38**, 240; (*b*) M. A. Woodruff and D. W. Hutmacher, *Prog. Polym. Sci.*, 2010, **35**, 1217; (*c*) T. Wu, Z. Wei, Y. Ren, Y. Yu, X. Leng and Y. Li, *Polym. Degrad. Stab.*, 2018, **155**, 173; (*d*) M. T. Hunley, N. Sari and K. L. Beers, *ACS Macro Lett.*, 2013, **2**, 375.
27 *CrysAlis PRO*, Rigaku Oxford Diffraction, 2017–2019.
28 G. M. Sheldrick, *Acta Crystallogr., Sect. A: Found. Adv.*, 2015, **71**, 3.
29 G. M. Sheldrick, *Acta Crystallogr., Sect. C: Struct. Chem.*, 2015, **71**, 3.
30 (*a*) P. v. d. Sluis and A. L. Spek, *Acta Crystallogr., Sect. A: Found. Crystallogr.*, 1990, **46**, 194; (*b*) A. L. Spek, *Acta Crystallogr., Sect. C: Struct. Chem.*, 2015, **71**, 9.